MEMORANDUM OF UNDERSTANDING

KRCE Society's

GGD Arts, BMP Commerce & SVS Science College, BAILHONGAL-591102

and

Department of collegiate Education

Government First Grade College, Gokak-591 307, Dist: Belagavi

for

RESEARCH COLLABORATIONS

This Memorandum of Understanding (MoU) is made between Shri N.K.Enagi, Assistant Professor department of Mathematics, KRCE Society'sGGD Arts, BMP Commerce & SVS Science College, BAILHONGAL-591102,District Belagaviand Dr.Sridhar Kulkarni, Assistant Professor, Department of Mathematics,Government First Grade College, Gokak-591307, District Belagavi.The purpose of this MoU is to inculcate research culture and attitude amongst the students and the teachers, each wishing to establish a cooperative research relationship through mutual interests in the areas of fluid mechanics.

Objectives of collaborative research activity:

a) To promote and enhance academic interest in research activities.

b) To carry out research activities on the research area of Fluid Mechanics.

c) Toestablish a joint research platform for publications in the research area.

This agreement will take effect from the date of its signing and shall be valid for the period of five years from that date unless sooner terminated, revoked or modified by mutual written agreement between the parties, and may be extended by mutual written agreement. Either party may terminate the agreement at any time during the term by the provision of three months written notice to the other party.
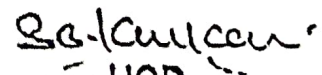
Signed to and on behalf of

Signed for and on behalf of

05·04·2018

Prof.N.K.Enagi

HEAD
Department of Mathematics
GGD Arts, BMP Commerce &
SVS Science College, Bailhongal

Dr.Sridhar Kulkarni
HOD
Department of Mathematics
G F G College Gokak.

5/4/20

PRINCIPAL,
K. R. C. E. Society's,
G, G. D. Arts, B. M. P. Commerce
S. V. S. Science College,
BAILHONGAL.

CO-ORDINATOR
I. Q. A. C. NAAC
BMP Commerce Bailhongal

PRINCIPAL
GOVT. FIRST GRADE COLLEGE
GOKAK. Belgaum Dt-591307

K.R.C.E.S's. G.G.D Arts, B.M.P
Commerce & S.V.S. Science

ON THE ONSET OF CONVECTION IN A COUPLE STRESS FLUID SATURATED ROTATING ANISOTROPIC POROUS LAYERS USING THERMAL NON-EQUILIBRIUM MODEL

Krishna B. Chavaraddi[1], N. K. Enagi[2,3] and Sridhar Kulkarni[4]

[1]S. S. Government First Grade College
P. G. Studies Center
Nargund 582 207
Karnataka, India

[2]Research and Development Centre
Bharathiar University
Coimbatore 641 046
India

[3]KRCE Society's GGD Arts
BMP Commerce and SVS Science Degree College
Bailhongal
India

[4]Government First Grade College
Gokak 591 307
Karnataka, India

Abstract

The onset of convection in a couple stress fluid saturated anisotropic rotating porous layer is investigated using linear stability analysis,

when the fluid and solid phases are not in local thermal equilibrium. The linear stability analysis is based on normal mode technique. It is assumed that the porous layer is anisotropic. It is also assumed that at the bounding surfaces the solid and fluid phases have identical temperatures. To study the effect of rotation a coriolis term, is incorporated in the momentum equation. A two field model equation each representing solid and fluid phase along with anisotropic term is used for energy equation. The linear stability theory is used to calculate the Rayleigh number for the onset of convection. The effect of couple stress parameter, anisotropic permeability and rotation on the onset of convection is shown graphically. It is found that the rotation, couples tress parameter and thermal anisotropy stabilize the system, whereas mechanical anisotropy destabilizes the system.

Nomenclature

a	Horizontal wave number, $\sqrt{l^2 + m^2}$
c	Specific heat
d	Height of the porous layer
g	Gravitational acceleration
K	Permeability tensor, $Kh(ii + jj) + Kzkk$
k_f	Thermal conductivity tensor of fluid phase
l, m	Wave numbers in the x and y direction, respectively
p	Pressure
q	Velocity vector, (u, v, w)
R_a	Rayleigh number, $\dfrac{\rho_0 \beta d(T_l - T_u)K}{\varepsilon K_f \mu_f}$
T	Temperature
t	Time
(x, y, z)	Space coordinates

Ta	Taylor number
H	Inter-phase heat transfer coefficient
C	Couple stress parameter

Greek symbols

α	Diffusive ratio
β	Coefficient of thermal expansion
γ	Porosity-modified conductivity ratio, $\dfrac{\varepsilon K_f}{(1-\varepsilon)K}$
ε	Porosity
ξ	Mechanical anisotropy parameter
η_f	Thermal anisotropy parameter for fluid phases
η_s	Thermal anisotropy parameter for solid phases
μ_e	Effective viscosity
μ_f	Fluid viscosity
μ	Dynamic viscosity
ϕ	Non-dimensional temperature of solid phase
θ	Non-dimensional temperature of fluid phase
ρ_f	Fluid density

Other symbols

∇_1^2	$\dfrac{\partial^2}{\partial x^2} + \dfrac{\partial^2}{\partial y^2}$
∇^2	$\nabla_1^2 + \dfrac{\partial^2}{\partial z^2}$

Subscripts/superscripts

l	Lower
s	Solid
c	Critical
f	Fluid phase
0	Reference
*	Dimensionless quantity

1. Introduction

One of the dominant and important mechanisms of heat transfer is convection. The study of convection in a fluid and fluid saturated porous medium has attracted considerable interest in recent year because of its importance in many practical fields such as chemical engineering, geothermal activities, oil recovery technique, building thermal insulation and biological processes. It is also of practical interest in the extraction of geothermal energy. The effective mixing process in petroleum reservoirs, regarded as fixed bed reactors is achieved by thermal convection. The study of convection has also great impact on many technological applications for example the evaluation of the amount of heat removal from a hypothetical accident in a nuclear reactor the prevention of convection and consequence freezing roads and railways providing effective insulation and so on.

The study of couple stress fluids has many applications such as extraction of polymer fluids, solidification of liquid crystals, cooling metallic plates in a bath, exotic lubrications and colloidal and suspension solutions. In the category of non-Newtonian fluids, couple stress fluids has a distinct feature, such as polar effects. The theory of polar fluids and related theories are models for fluids whose microstructure is mechanically significant. Couple stress found to be appeared in noticeable magnitude in fluids with very large molecules.

Anisotropy is generally a consequence of preferential orientation or

asymmetric geometry of porous matrix or fibers. An excellent review of research on convective flow through anisotropic porous media has recently been well documented by McKibbin [34] and Storesletten [22].

Most of the works on convective instability in porous media have mainly been investigated under the assumption that the fluid and porous medium are everywhere in local-thermal equilibrium (LTE). However, in many practical applications the solid and fluid phases are not in local thermal equilibrium. Nield and Bejan [2] have discussed a two field model for energy equation. Instead of having a single energy equation, which describes the common temperature of the saturated porous media, two equations are used for fluid and solid phase separately. In two-field model, the energy equations are coupled by the terms, which account for the heat lost or gained from the other phase. Rees and co-workers [8, 9] in a series of studies have investigated thermal non-equilibrium (LTNE) effect on free convective flows in porous medium. The effect of mechanical and thermal anisotropy on the stability of gravity driven convection in rotating porous media in the presence of thermal non-equilibrium model was investigated by Govender and Vadasz [36]. Research on thermal non-equilibrium in porous media is provided by Banu and Rees [31] and Malashetty et al. [23-29] whilst Kuznetsov [5] provides a detailed review of work on thermal non-equilibrium effects on convection in porous media. The onset of a Darcy-Brinkman convection using a thermal non-equilibrium model has been studied by Postelnicu [3]. Kuznetsov and Nield [4] have investigated the effect of local thermal non-equilibrium on the onset of convection in a porous medium saturated by a nano fluid. Recently Srivastava et al. [2] investigated magnetoconvection in an anisotropic porous layer using thermal non-equilibrium model. A detailed study on thermal non-equilibrium model has been carried out by Shivakumara et al. [11-18].

The study of effect of local thermal non-equilibrium on the stability of natural convection in an oldroyd-B fluid saturated vertical porous layer is carried out by Shankar and Shivakumar [6].

The external rotation of the fluid or fluid-saturated porous layer is one of

the convenient and effective mechanisms to control the onset of convection. A possible engineering application of the findings of the current study could include the cooling of electronic circuits found in rotating radars. In this paper, we study the onset of convection in a couple-stress fluid saturated rotating anisotropic porous layer heated from below with emphasis on how the condition for the onset of convection is modified by LTNE, anisotropy and rotation.

2. Mathematical Formulation

We consider a couple-stress fluid saturated anisotropic rotating porous layer of depth d, which is heated from below and cooled from above. The lower surface is held at a temperature T_1, while the upper surface is at T_u. We assume that the solid and fluid phases of the medium are not in local thermal equilibrium and use a two-field model for temperatures. The basic governing equations are

$$\nabla \cdot q = 0, \tag{1}$$

$$\frac{2}{\varepsilon}\Omega \times q = -\nabla p - \frac{1}{K}\left(\mu_f - \mu_e \nabla^2\right)q + \rho_f g, \tag{2}$$

$$(\rho_c)_f q \cdot \nabla T_f = \varepsilon K_{fh}\nabla^2 T_f + h(T_s - T_f), \tag{3}$$

$$(1 - \varepsilon)K\nabla T - h(T_s - T_f) = 0, \tag{4}$$

$$\rho_f = \rho_0\left[1 - \beta(T_f - T_u)\right]. \tag{5}$$

We eliminate the pressure from the momentum equation and render the resulting equation and the energy equations for fluid phase and solid phase dimensionless by using the following transformations:

$$(x, y, z) = d(x^*, y^*, z^*)(u, v, w) = \varepsilon\frac{K_f}{(\rho_c)_f d}(u^*, v^*, w^*)p = \varepsilon\frac{K_f \mu}{(\rho_c)_f K}\rho^*,$$

$$T_f = (T_l - T_u)\theta_f^* + T_u, \quad T_s = (T_l - T_u)\phi^* + T_u, \quad t = \varepsilon\frac{(\rho_c)_f d^2}{K_f}t^*. \tag{6}$$

Equations (2)-(4) take the following form:

$$\left[\left(\nabla^2 - C\nabla^4 + \frac{1}{\xi}\frac{\partial^2}{\partial z^2}\right)\right]w + T_a \frac{\partial^2 w}{\partial z^2}\partial^2 w = R_a T_f, \tag{7}$$

$$(q \cdot \nabla)T_f = \eta_f \nabla_1^2 T_f + \frac{\partial^2 T_f}{\partial z^2} + H(T_s - T_f), \tag{8}$$

$$\eta_s \nabla^2 T_s + \frac{\partial^2 k}{\partial z^2} - \gamma H(T_s - T_f), \tag{9}$$

$$\left. \begin{array}{l}
R_a = \dfrac{\rho_f g \beta (T_l - T_u)K_z d}{\varepsilon \mu_f K_f}, \qquad\qquad \gamma = \dfrac{\varepsilon k_f}{(1-\varepsilon)k_s}, \quad H = \dfrac{hd^2}{\varepsilon k_{fz}}, \\[3mm]
\alpha = \dfrac{(\rho_c)_s}{(\rho_c)_f}\dfrac{k_f}{k_z} = \dfrac{K_f}{K_z}, \qquad\qquad \eta_s = \dfrac{k_{sh}}{k_{sz}}, \qquad \eta_f = \dfrac{k_{fh}}{k_{fz}}, \ \xi = \dfrac{K_h}{K_z} \\[3mm]
Ta = \left(\dfrac{2\Omega K \rho_o}{\varepsilon \mu_f}\right)^2, \ \text{the Taylor number}
\end{array} \right\}. $$

$$\tag{10}$$

(The asterisks have been dropped for simplicity.)

3. Basic State

The basic state is assumed to be quiescent and is given by

$$u = v = w = 0, \quad T_f = T_{fb}(z), \quad T_s = T_{sb}(z). \tag{11}$$

The basic state temperatures of fluid phase and solid phase satisfy the equations

$$\frac{d^2 T_{fb}}{dz^2} + H(T_{sb} - T_{fb}) = 0, \tag{12}$$

$$\frac{d^2 T_{fb}}{dz^2} - \gamma H(T_{sb} - T_{fb}) = 0 \tag{13}$$

with boundary conditions

$$T_{fb} = T_{sb}(z) = 1, \quad at z = 0, \quad T_{fb} = T_{sb}(z) = 0 \quad \text{at} \quad z = 1 \qquad (14)$$

so that the conduction state solutions are given by

$$T_{fb} = T_{sb}(z) = (1 - z). \qquad (15)$$

The basic state is perturbed and the quantities in the perturbed state are given by

$$(u, v, w) = (u^1, v^1, w^1), \quad T_f = T_{fb} + \theta, \quad T_s = T_{sb} + \phi. \qquad (16)$$

Substituting equations (16) into equations (7)-(9) and using the basic state solutions, we obtain the following equations for the perturbed quantities (after neglecting the primes)

$$\xi\nabla^2 w - \xi C\nabla^4 w + \frac{\partial^2 w}{\partial z^2} + \xi T_a \frac{\partial^2 w}{\partial z^2} - Ra\nabla_1^2\theta = 0, \qquad (17)$$

$$\eta_s\nabla_1^2\phi + \frac{\partial^2\phi}{\partial z^2} - \gamma H(\phi - \theta) = 0, \qquad (18)$$

$$q.\nabla\theta + w' = \eta_f\nabla_1^2\theta + \frac{\partial^2\theta}{\partial z^2} + H(\phi - \theta). \qquad (19)$$

Since the fluid and solid phases are not in local thermal equilibrium, the use of appropriate thermal boundary conditions may pose a difficulty. However, the assumption that the solid and fluid phases have equal temperatures at the bounding surfaces made at the beginning of this section helps in overcoming this difficulty. Accordingly, equations (17) to (19) are solved for impermeable isothermal boundaries. Hence the boundary conditions are

$$\left. \begin{array}{l} w = 0 \quad \text{at} \quad z = 0, 1 \\ \theta = \phi = 0 \quad \text{at} \quad z = 0, 1 \end{array} \right\}. \qquad (20)$$

4. Linear Stability Theory

To study the linear stability theory, we use the linearized version of

equations (17)-(19). The principle of exchange of stabilities holds in the presence of anisotropy and non-LTE effects (there is only one destabilizing agency) so that the onset of convection is stationary.

We seek the solutions to the linearized equations in the form

$$[w,\ \theta,\ \phi] = [A_1,\ A_2,\ A_3]\exp i(lx + my)\sin \pi z, \tag{21}$$

where A's are constants. Substituting equations (21) in equations (17)-(19) we obtain the following matrix equation:

$$
\begin{bmatrix}
\xi a^2 + \xi C(a^2 + \pi^2)^2 + (1+\xi T_a)\pi^2 & -R_a a^2 & 0 \\
1 & -(\pi^2 + a^2\eta_f + H) & H \\
0 & \gamma H & -(\pi^2 + a^2\eta_s + \gamma H)
\end{bmatrix}
$$

$$
\cdot\begin{bmatrix} A_1 \\ A_2 \\ A_3 \end{bmatrix} = \begin{bmatrix} 0 \\ 0 \\ 0 \end{bmatrix}. \tag{22}
$$

By setting the determinant of the above matrix to zero we get

$$
Ra = \left[\frac{\xi a^2 + \xi C(a^2 + \pi^2)^2 + (1+\xi T_a)\pi^2}{\xi a^2}\right]\left[\pi^2 + a^2\eta_f - \frac{H(\pi^2 + a^2\eta_s)}{\pi^2 + a^2\eta_f + H}\right]. \tag{23}
$$

5. Results and Discussion

Figures 1(a) to 1(f) show neutral curves for various parameter values. From these figures it is clear that the neutral curves are topologically connected. This connectedness allows the linear stability criteria to be expressed in terms of the critical Rayleigh number below which the system is stable and unstable above. Figure 1(a) shows that the effect of rotation on neutral curves. It is observed that the minimum Rayleigh number increases with increase in rotation indicating the effect of rotation is to stabilize the system. Figure 1(b) shows the effect of conductivity ratio γ on neutral curves.

It is evident that the minimum Rayleigh number decreases with increase in γ which shows that the conductivity ratio γ destabilizes the system.

Figure 1(c) shows that the effect of couple stress parameter on neutral curves. In this case, the increase in Rayleigh number increases with increase in couple stress parameter indicating the effect of couple stress parameter is to stabilize the system.

The effects of the thermal anisotropy parameters η_s and η_f for fluid and solid phases on neutral curves are shown in Figures 1(d) and 1(e). The minimum Rayleigh number increases with increase in η_s and η_f. Thus the effect of increase in η_s and η_f delays the onset of convection. It is also seen that the effect of thermal anisotropy of fluid phase is more pronounced than that of the solid phase on the stability characteristics. Figure 1(f) shows the neutral curves for different values of mechanical anisotropic parameter ξ. It is found that the minimum Rayleigh number decreases with increase in ξ. Thus the mechanical anisotropy has destabilizing effect on the onset of convection.

Figure 2(a) shows graph of critical Rayleigh number verses inter phase heat transfer coefficient H for a range of values of the parameters T_a. We observe that the critical Rayleigh number is constant for vary small and large values of H. But for modular values of H critical Rayleigh number increases with increase in T_a which shows that the effect of T_a makes the system more stable. Figure 2(b) represents the effect of conductivity ratio γ on critical Rayleigh number. It is found that the critical Rayleigh number increases with increase in γ indicating the conductivity ratio enhances the stability of the system. It is also observed that the critical Rayleigh number is independent of γ for very small values of H. This is because for very small values of H there is almost no transfer of heat between the phases.
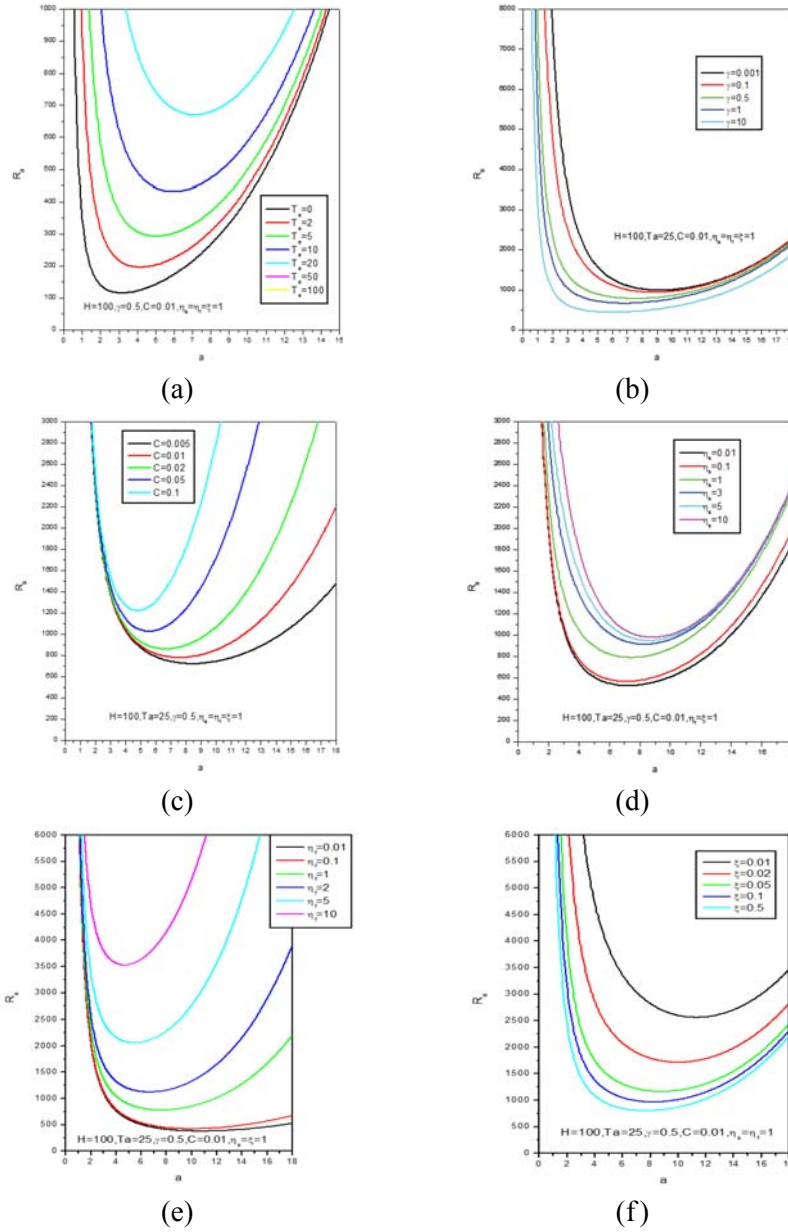
Figure 1 (a)-(f). Neutral curves for different values of (a) Taylor number *Ta*, (b) conductivity ratio γ, (c) couple stress parameter *C*, (d) thermal anisotropy for fluid phase η_f, (e) thermal anisotropy for solid phase η_s and (f) mechanical anisotropy ξ.
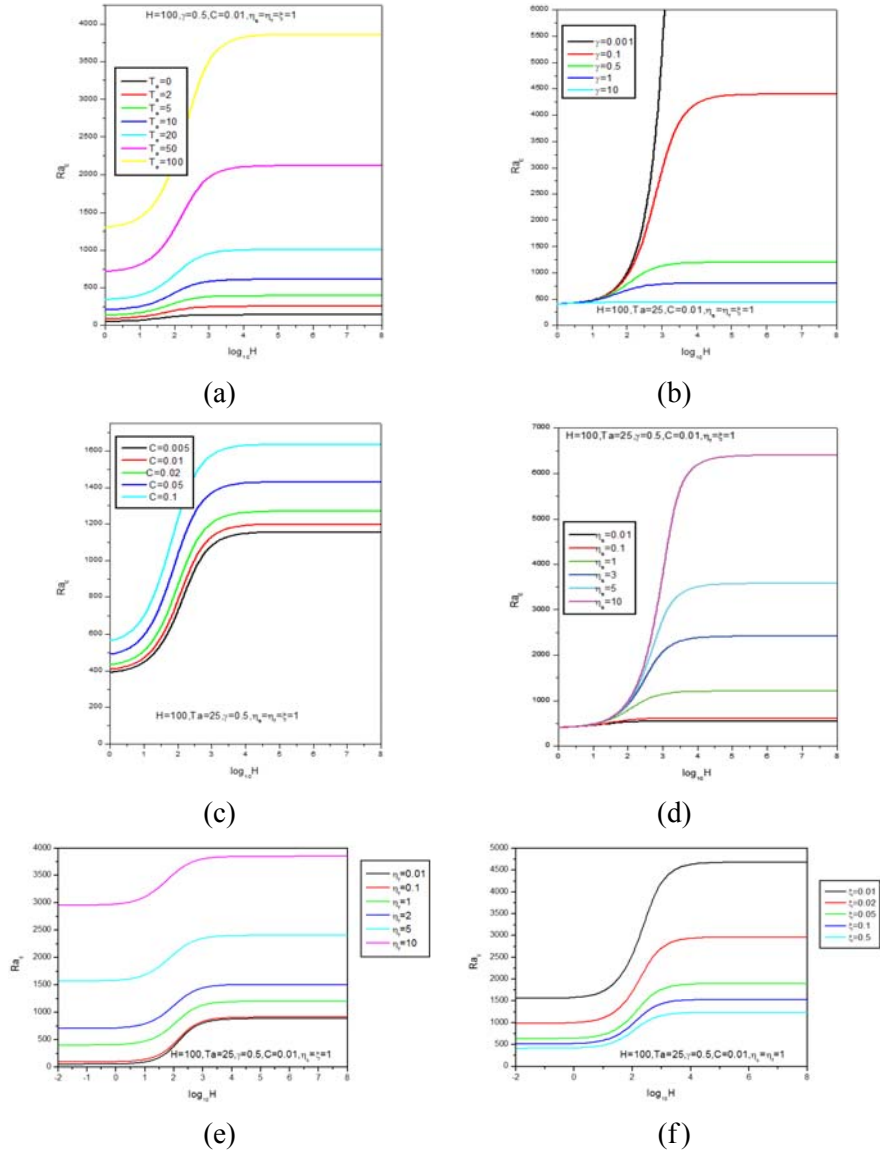
Figure 2 (a)-(f). Variation of critical Rayleigh number with interphase heat transfer coefficient *H* for different values of (a) Taylor number *Ta*, (b) conductivity ratio γ, (c) couple stress parameter *C*, (d) thermal anisotropy for fluid phase η_f, (e) thermal anisotropy for solid phase η_s and (f) mechanical anisotropy ξ.

The effect of couple stress parameters on critical Rayleigh number is displayed in Figure 2(c). It is observed that with increase in couple stress parameters, critical Rayleigh number increases, which shows that the couple stress parameter C has the stabilizing effect on the onset of convection. The effects of thermal anisotropy parameter for both fluid and solid phases are displayed in Figures 2(d) and (e). It is found that R_{ac} in both cases are found to increase with increases in η_f and η_s indicating the effect of these parameters η_f and η_s is to stabilize the system.

The effect of ξ on critical Rayleigh number is displayed in Figure 2(f). It is found that critical Rayleigh number R_{ac} decreases with increase in ξ. It is also noted that for very small values of H, R_{ac} is constant and increases slowly and reaches maximum, then it reaches asymptotic values for large H depending on the value of ξ. Let us keep the vertical permeability K_z fixed (or the horizontal permeability K_h fixed) and vary the horizontal permeability K_h (or the vertical permeability). Then the increased horizontal permeability reduces the Rayleigh number, indicating that the system becomes unstable. The effect of the anisotropic parameter is more significant for $\xi < 1$.

Figures 3(a)-(f) show the critical curves of critical wave number verses interphase heat transfer coefficient H for a range of values of Ta, γ, C, η_s, η_f and ξ. In these figures we see that the critical wave number is constant for very small and large values of H. This is because the solid phase ceases to affect the thermal field of the fluid when $H \to 0$ and on the other hand, the solid and fluid phases will have identical temperatures when $H \to \infty$. For the intermediate values of H, the critical wave number attains maximum value for each of the parameters Ta, γ, C, η_s, η_f and ξ. It is also noted that approaches a common limit as $H \to 0$ and $H \to \infty$ in the case of γ. But in all other cases critical wave number does not approach to common limits as $H \to 0$ and as $H \to \infty$.
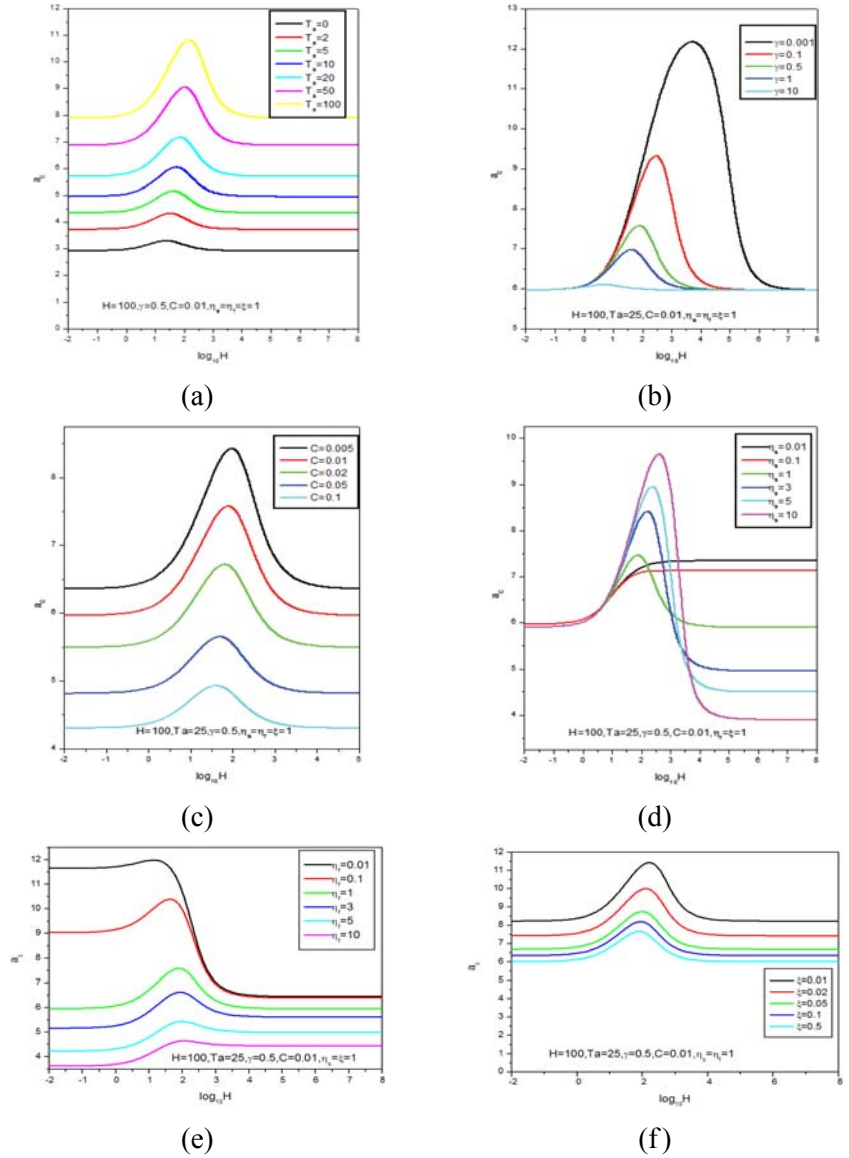
(a)

(b)

(c)

(d)

(e)

(f)

Figure 3 (a)-(f). Variation of critical wave number with interphase heat transfer coefficient H for different values of (a) Taylor number Ta, (b) conductivity ratio γ, (c) couple stress parameter C, (d) thermal anisotropy for fluid phase η_f, (e) thermal anisotropy for solid phase η_s and (f) mechanical anisotropy ξ.

6. Conclusion

The onset of convection in a couple-stress fluid saturated anisotropic rotating porous layer using thermal non-equilibrium model is investigated. It is found that the increase in rotation *Ta* makes the system more stable, whereas increase in conductivity ratio γ destabilizes the system. The effect of increasing couple-stress parameter *C* and thermal anisotropy parameter η_s, η_f delay the onset of convection. The mechanical anisotropy parameter ξ has a destabilizing effect on the onset of convection.

Acknowledgement

References

[1] A. K. Goel and S. C. Agarwal, Hydromantic stability of an unbounded couple stress binary fluid mixture having vertical temperature and concentration gradients with rotation, Indian J. Appl. Math. 30(10) (1999), 991-1001.

[2] A. K. Srivastava, B. S. Bhadauria and Jogendra Kumar, Magnetoconvection in an anisotropic porous layer using thermal non-equilibrium model, Special Topics & Reviews in Porous Media 1(2) (2011), 1-10.

[3] A. Postelnicu, Effect of Inertia on the onset of mixed convection in a porous layer using thermal non-equilibrium model, J. Porous Media 10(5) (2007), 515-524.

[4] A. V. Kuznetsov and D. A. Nield, Effect of local thermal non-equilibrium on the onset of convection in a porous medium layer saturated by a nanofluid, Transport in Porous Media 2(83) (2010), 425-436.

[5] A. V. Kuznetsov, Thermal non-equilibrium forced convection in porous media, Transport Phenomena in Porous Media, Derek B. Ingham and I. Pop, eds., Pergamon, Oxford, 1998, pp. 103-130.

[6] B. M. Shankar and I. S. Shivakumar, Effect of local thermal non-equilibrium on the stability of natural convection in an Oldroyd-B fluid saturated vertical porous layer, J. Heat Transfer 139(4) (2017), 1-10.

[7]   D. A. Nield and A. Bejan, Convection in Porous Media, 3rd ed., Springer, Berlin, 2006.

[8]   D. A. S. Rees and I Pop, Free convection in stagnation point flow in a porous medium using thermal non equilibrium model, Int. Con. Heat Mass Transfer 26 (1999), 945-954.

[9]   D. A. S. Rees, L. Storesletten and A. Postelnicu, The onset of convection in an inclined anisotropic porous layer with oblique principle axes, Transport in Porous Media 62(2) (2006), 139-156.

[10]   D. B. Ingham and I. Pop, Transport Phenomena in Porous Media, Elsevier, Oxford, 2005.

[11]   I. S. Shivakumara, M. S. Malashetty and K. B. Chavaraddi, Onset of convection in a viscoelastic-fluid-saturated sparsely packed porous layer using a thermal nonequilibrium model, Canadian J. Physics 84(11) (2006), 973-990.

[12]   I. S. Shivakumara, A. L. Mamatha and M. Ravisha, Boundary and thermal nonequilibrium effects on the onset of Darcy-Brinkman convection in a porous layer, J. Engin. Math. 67 (2010), 317-328.

[13]   I. S. Shivakumara, A. L. Mamatha and M. Ravisha, Effects of variable viscosity and density maximum on the onset of Darcy-Benard convection using a thermal nonequilibrium model, J. Porous Media 13(7) (2010), 613-622.

[14]   Jinho Lee, I. S. Shivakumara and M. Ravisha, Effect of thermal non-equilibrium on convective instability in a ferromagnetic fluid saturated porous medium, Transport in Porous Media 86 (2011), 103-124.

[15]   I. S. Shivakumara, Jinho Lee, M. Ravisha and R. Gangadhara Reddy, The onset of Brinkman ferroconvection using a thermal non-equilibrium model, Inter. J. Heat and Mass Transfer 54 (2011), 2116-2125.

[16]   I. S. Shivakumara, Jinho Lee, A. L. Mamatha and M. Ravisha, Boundary and thermal non-equilibrium effects on convective instability in an anisotropic porous layer, J. Mech. Sci. Tech. 25 (2011), 911-921.

[17]   I. S. Shivakumara, R. Gangadhara Reddy, M. Ravisha and Jinho Lee, Effect of rotation on ferromagnetic porous convection with a thermal non-equilibrium model, Meccanica 49 (2014), 1139-1157.

[18]   I. S. Shivakumara, M. Ravisha, Chiu-On Ng and V. L. Varun, A thermal nonequilibrium model with Cattaneo effect for convection in a Brinkman porous layer, Inter. J. Nonlinear Mech. 71 (2015), 39-47.

[19] K. Sridhar, Darcy Brinkman convection in a couple stress fluid saturated rotating porous layer using thermal non equilibrium model, J. Global Research Math. Arch. 1(8) (2013), 16-33.

[20] K. Sridhar, The unsteady thermal convection in a Maxwell fluid saturated porous layer using thermal non-equilibrium model, Inter. J. Math. Arch 5(8) (2014), 222-234.

[21] K. Sridhar, Unsteady thermal convection in a rotating anisotropic porous layer using a thermal non equilibrium model, Inter. J. Phys. Math. Sci. 3(3) (2013), 30-46.

[22] L. Storesletten, Effects of anisotropy on convective flow through porous media, Transport Phenomena in Porous Media, D. B. Ingham and I. Pop, eds., Pergamon Press, Oxford, 1998, pp. 261-283.

[23] M. S. Malashetty, I. S. Shivakumara and Sridhar Kulkarni, Convective instability of Oldroyd-B fluid saturated porous layer heated from below using a thermal nonequilibrium model, Transport in Porous Media 64 (2006), 123-139.

[24] M. S. Malashetty, I. S. Shivakumara and Sridhar Kulkarni, The onset of convection in an anisotropic porous layer using a thermal non-equilibrium model, Transport in Porous Media 51 (2005), 1-17.

[25] M. S. Malashetty, I. S. Shivakumara and Sridhar Kulkarni, The onset of convection in a couple stress fluid saturated porous layer using a thermal non-equilibrium model, Physics Letters A 373 (2009), 781-790.

[26] M. S. Malashetty, I. S. Shivakumara and Sridhar Kulkarni, The onset of Lapwood-Brinkman convection using a thermal non-equilibrium model, Inter. J. Heat Mass Transfer 48(6) (2005), 1155-1163.

[27] M. S. Malashetty, I. S. Shivakumara and Sridhar Kulkarni, The onset of convection in a couple stress fluid saturated porous layer using a thermal non-equilibrium model, Physics Letters A 373(7) (2009), 781-790.

[28] M. S. Malashetty, Mahantesh Swamy and Sridhar Kulkarni, Thermal convection in a rotating porous layer using a thermal nonequilibrium model, Physics of Fluids 19(5) (2007), 054102.

[29] M. S. Malashetty, I. S. Shivakumar and Sridhar Kulkarni, The onset of convection in an anisotropic porous layer using a thermal non equilibrium model, Transport in Porous Media 60 (2004), 199-215.

[30] M. S. Malashetty, A. A. Hill and Mahantesh Swamy, Double diffusive convection in a visco elastic fluid saturated porous layer using a thermal non equilibrium model, Acta Mech. 223 (2012), 967-983.

[31] N. Banu and D. A. S. Rees, Onset of Darcy-Benard convection using a thermal non-equilibrium model, Int. J. Heat Mass Transfer 45 (2002), 2221-2228.

[32] I. S. Shivakumara, A. L. Mamatha and M. Ravisha, Local thermal non-equilibrium effects on thermal convection in a rotating anisotropic porous layer, Appl. Math. Comput. 259 (2015), 838-857.

[33] P. A. Tyvand and L. Storesletten, Onset of convection in an anisotropic porous medium with oblique principal axes, J. Fluid Mech. 226 (1991), 371-382.

[34] R. McKibbin, Thermal convection in a porous layer: effects of anisotropy and surface boundary conditions, Transport in Porous Media 1(3) (1986), 271-292.

[35] S. Govender, On the effect of anisotropy on the stability of convection in rotating porous media, Transport in Porous Media September 64(3) (2006), 413-422.

[36] S. Govender and P. Vadasz, The effect of mechanical and thermal anisotropy on the stability of gravity driven convection in rotating porous media in the presence of thermal non-equilibrium, Transport in Porous Media 69(1) (2007), 55-66.

[37] V. K. Stokes, Couple-stress in fluids, Phys. Fluids 9 (1966), 1709-1715.

Research article

Effect of maximum density and internal heating on the stability of rotating fluid saturated porous layer using LTNE model

N.K. Enagi [a,b], Krishna B. Chavaraddi [c,*], Sridhar Kulkarni [d], G.K. Ramesh [e]

[a] University: Research and Development Centre, Bharathiar University, Coimbatore-641046, India
[b] Department of Mathematics, KRCE Society's GGD Arts, BMP Commerce and SVS Science College, Bailhongal-591102, India
[c] Department of Mathematics, S.S. Government First Grade College & P.G. Studies Center, Nargund-582207, India
[d] Department of Mathematics, Government First Grade College, Gokak-591307, India
[e] Department of Mathematics, K.L.E. Society's J.T. College, Gadag-582101, India

A B S T R A C T

The impact of heat generated inside the porous layer containing a fluid and density maximum when the porous structure is studied analytically subjected to rotation for the case of unlike temperatures of both solid and fluid phases. Two equations each representing solid and fluid phases are used as energy equations. The linear stability theory is used and is based on normal mode technique. Galerkin method is used to find the Eigen values of the problem. The rotation of the porous layer provides extra strength to the system, protecting the structure from instability, however internal heat generation does not support the system in retaining its strength, causing the system to destabilize. Both the conductivity ratio and the density function have a negative impact on system stability. Consequently, the rotation parameter Ta stabilizes the system, whereas internal heat generation, conductivity ratio, and density function destabilizes the onset of convection.

1. Introduction

Convective heat transfer is one of the most influenced and powerful mechanism. The study of convective heat transfer in a porous medium containing fluid has gained much attention in these days, because of its vital importance in extraction of energy from the surface of the earth. It is found that in most of the cases the source of heat is generated by taking itself which leads to setting up of convection by the generation of heat inside the layer. In most of natural and practical context in which convection is managed by internal heat sources. Hence the study of internal heat generation acquired much significance, because its applications include the storage of radioactive materials, geophysics and combustion.

Nield and Bejan [1] have introduced a model of energy which has two equations is called a two-fluid model. Rees [2, 3] in his paper studied through a porous medium when the solid and fluid phases have different temperatures. Govender and Vadasz [4] examined stability of anisotropic rotating, driven convection in the layer. The most important investigation on thermal stability in porous media is well documented by Banu and Rees [5] and Malashetty et al. [6, 7, 8, 9, 10]. Postelnicu [11] has been investigated the stability of convection by using Darcy-Brinkman model. Kuznetsov et al. [12] all have analyzed how the convection in nanofluid saturated in the permeable medium is affected when both fluid and solid phases have different temperature.

Yekasi et al. [13] has explored the characterization of heating inside on Rayleigh-Benard convection driven by suction-injection combination by considering free rigid boundary. Bhaduria et, al [14] investigated how the time periodic gravity modulation with inside heating on Rayleigh-Benard convection in vertically oscillating micro polar fluid. A detailed study on thermal non-equilibrium model has been carried out by Shivakumara et al. [15, 16, 17, 18, 19, 20, 21, 22]. Dhananjay Yadav et al. [23] examined the effect of inner heating and rotating layer using Darcy–Brinkman model and conclude that rotation inhibits the system. Sarvanan [24] has studied the nature of internal heat generation and maximum density function and
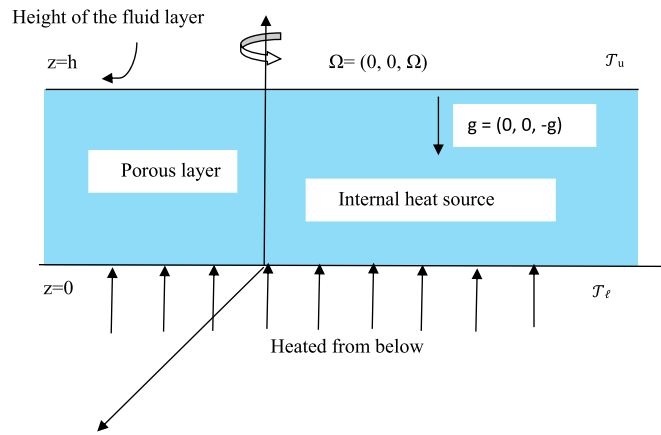

Fig. 1. Physical configuration.

shows that both the parameters enhance the stability of the system. Gaseer et al. [25] studied the effect interior heating for the onset of convection. Chavaraddi et al. [26] gave a conclusion that the couple stress, rotation and thermal anisotropy parameters are stabilizing the onset of convection in a saturated medium. Lotten and Rees [27] studied the anisotropy and heat generated inside in an inclined layer. Israel-Cookey and Omubo-Peppl [28] studied the stability in a low Prandtl number fluid with heating process inside the structure. Srivastava et al. [29] examined the onset of thermal magneto convection in an anisotropic loosely pack medium. Postelnicu [30] studied the effect of inertia on the onset of mixed convection in LTNE medium. Xu et al. [31] focuses on various flow and heat transfer modes of nanofluid, metal foam and the combination of the two, with the physical properties of nanofluid and metal foam summarized. Oumar et al. [32] have been studied the onset of Rayleigh-Benard electro-convection in a micro polar fluid with internally heating particles. A new fractal theoretical model with periodic pore morphology, which idealizes the pore channels of the porous media as gourd-shaped structure, is established to model the transport in complex porous media by Wu et al. [33]. Xu [34] investigated the theoretical study of the fully-developed forced convection heat transfer in a microchannel partially filled with a porous medium core is performed by considering the local thermal non-equilibrium (LTNE) effect between the solid and fluid phases. Anwar Ahmed Yousif et al. [35] investigated the impact of using triple adiabatic obstacles on natural convection inside porous cavity under non-Darcy flow and local thermal non-equilibrium model. Omar Rafae et al. [36, 37, 38] examined the simulation of complete liquid–vapor phase change process inside porous evaporator using local thermal non-equilibrium model.

In most of the situations it is observed that temperature fields of solid and fluid phase of the porous medium are assumed to be identical such a situation is generally known as local thermal equilibrium (LTE). However, in many practical situations involving porous material and also media in which there is a large temperature difference between the fluid and the solid phases, it has been realized that the assumption of LTE model is inadequate for proper understanding of the heat transfer problems. In such circumstances the local thermal non-equilibrium (LTNE) effects are to be taken into consideration in which case the single energy equation has to be replaced by two, one for each phase. The main objective of present paper is to study the effect of maximum density and internal heating on the stability of rotating fluid using LTNE model.

2. Mathematical model

In this paper, we consider a porous media of height 'h' which is extended horizontally between two free surfaces and the fluid is subjected to rotation. Let T_ℓ and $\mathcal{T}_u$ be the temperatures at the lower and upper surfaces. The temperature gradient $\nabla \mathcal{T} = \mathcal{T}_\ell - \mathcal{T}_u$ is uniform and $\mathcal{T}_\ell > \mathcal{T}_u$ maintained between the two surfaces. A momentum expression contains the time derivative term and two separate equations are used for temperature. This physical model is shown in Fig. 1.

$$\nabla \cdot q = 0 \tag{1}$$

$$\frac{1}{\varepsilon}\frac{\partial q}{\partial t} + \frac{2}{\varepsilon}\Omega \times q = -\frac{1}{\rho_o}\nabla p + \frac{\rho}{\rho_o}g - \frac{v}{k}q \tag{2}$$

$$\varepsilon(\rho_c)_f \frac{\partial T_f}{\partial t} + (\rho_c)_f (q \cdot \nabla)\mathcal{T}_f = \varepsilon k_f \nabla^2 \mathcal{T}_f + h(\mathcal{T}_s - \mathcal{T}_f) + \varepsilon q_f \tag{3}$$

$$(1-\varepsilon)(\rho_c)_s \frac{\partial T_s}{\partial t} = (1-\varepsilon)k_s \nabla^2 \mathcal{T}_s - h(\mathcal{T}_s - \mathcal{T}_f) + (1-\varepsilon)q_s \tag{4}$$

$$\rho = \rho_0[1 - \beta_1(\mathcal{T}_f - \mathcal{T}_u) - \beta_2(\mathcal{T}_f - \mathcal{T}_u)^2 \tag{5}$$

To remove the pressure term from the momentum equation (2) and making equations (3) and (4) dimensionless by using eq. (5) and following transformations (6):

$$\left.\begin{array}{l} (x, y, z) = d(x^*, y^*, z^*) \qquad (u, v, w) = \frac{\varepsilon k_f}{(\rho_c)_f d}(u^*, v^*, w^*)\, p = \frac{k_f \mu}{(\rho_c)_f K}p^*, \\[3mm] \mathcal{T}_f = (\mathcal{T}_l - \mathcal{T}_u)\mathcal{T}_f^* + \mathcal{T}_u, \quad \mathcal{T}_s = (\mathcal{T}_l - \mathcal{T}_u)\mathcal{T}_s^* + \mathcal{T}_u, \quad t = \frac{(\rho_c)_f d^2}{k_f}t^* \end{array}\right\} \tag{6}$$

$$\frac{1}{P_{rD}}\frac{\partial}{\partial t}(\nabla^2 w) + (T_a)^{1/2}\frac{\partial^2 w}{\partial z^2} = R_1 \nabla_1^2 \mathcal{T}_f + R_2 \nabla_1^2 \mathcal{T}_f^2 - \nabla_1^2 w - \frac{\partial^2 w}{\partial z^2} \tag{7}$$

$$\frac{\partial T_f}{\partial t} + w \frac{\partial^2 T_f}{\partial z^2} = \nabla_1^2 \mathcal{T}_f + \frac{\partial^2 T_f}{\partial z^2} + H\left(\mathcal{T}_s - \mathcal{T}_f\right) + Q_f \tag{8}$$

$$\alpha \frac{\partial T_s}{\partial t} = \nabla_1^2 \mathcal{T}_s + \frac{\partial^2 T_s}{\partial z^2} - \gamma H\left(\mathcal{T}_s - \mathcal{T}_f\right) + Q_s \tag{9}$$

$$R_A = \beta_1 \rho_0 g h (\rho_c)_f \left(\mathcal{T}_l - \mathcal{T}_u\right) K / \varepsilon \mu k_f, \qquad R_M = \beta_2 \rho_0 g h (\rho_c)_f \left(\mathcal{T}_l - \mathcal{T}_u\right)^2 K / \varepsilon \mu k_f \tag{10}$$

Here Eq. (10) is the Rayleigh number corresponding to the properties of fluid phase.
Here R_M serves as a measure of the density maximum and when to begin property.

$$H = hd^2/(1-\varepsilon) k_s, \text{ the non-dimensional interphase heat transfer coefficient} \tag{11}$$

$$Ta = 2\Omega \rho_o K / \varepsilon \mu, \text{ the Taylor number} \tag{12}$$

$$\gamma = \varepsilon k_f/(1-\varepsilon) k_s, \text{ the conductivity ratio} \tag{13}$$

$$\alpha = (\rho_c)_s k_f/(\rho_c)_f k_s, \text{ the diffusivity ratio} \tag{14}$$

$$Q_f = q_f/\left(\mathcal{T}_l - \mathcal{T}_u\right) k_f, \text{ the fluid phase internal heat generator parameter} \tag{15}$$

$$Q_s = d^2 q_s/\left(\mathcal{T}_l - \mathcal{T}_u\right) k_s \text{ solid phase internal heat generator parameters} \tag{16}$$

where Eqs. (11)-(13) are Taylor number, conductivity ratio and diffusivity ratio respectively.

2.1. Quiescent state

The basic state is assumed to be quiescent and is given by

$$u = v = w = 0 \qquad \mathcal{T}_f = \mathcal{T}_{fb}(z) \qquad \mathcal{T}_s = \mathcal{T}_{sb}(z) \tag{17}$$

The temperature of fluid phase and solid phase satisfies the equations

$$\frac{d^2 T_{fb}}{dz^2} = -Q_f, \qquad \frac{d^2 \mathcal{T}_{sb}}{dz^2} = -Q_s \tag{18}$$

with the boundary conditions $\mathcal{T}_{fb} = \mathcal{T}_{sb} = 1$ at $z = 0$ $\mathcal{T}_{fb} = \mathcal{T}_{sb} = 0$ at $z = 1$ \hfill (19)

So that the steady state solutions are given by

$$T_{fb} = -\frac{Q_f}{2} z^2 + \left(\frac{Q_f}{2} - 1\right) z + 1, T_{sb} = -\frac{Q_s}{2} z^2 + \left(\frac{Q_s}{2} - 1\right) z + 1 \tag{20}$$

2.2. Perturbed state

The basic state is perturbed and quantities in the perturbed state are given by

$$(u, v, w) = \left(u^1, v^1, w^1\right), \quad q = q^1, \quad \mathcal{T}_f = \mathcal{T}_{fb} + \theta, \quad \mathcal{T}_s = \mathcal{T}_{sb} + \varphi \tag{21}$$

Substituting equation (21) into (7) to (9) and using equation (20) we obtained following linearized equations for perturbed quantities (after neglecting the primes)

$$\frac{1}{P_{rD}} \frac{\partial}{\partial t} (\nabla^2 w) + (T_a)^{1/2} \frac{\partial^2 w}{\partial z^2} = R_A \nabla_1^2 \theta + 2R_M \left\{ -Q_f \frac{z^2}{2} + \left(\frac{Q_f}{2} - 1\right) z + 1 \right\} \nabla_1^2 \theta - \nabla_1^2 w - \frac{\partial^2 w}{\partial z^2} \tag{22}$$

$$\frac{\partial \theta}{\partial t} + w \left(-Q_f z + \frac{Q_f}{2} - 1\right) = \nabla_1^2 \theta + \frac{\partial^2 \theta}{\partial z^2} + H(\varphi - \theta) \tag{23}$$

$$\alpha \frac{\partial \varphi}{\partial t} = \nabla_1^2 \varphi + \frac{\partial^2 \varphi}{\partial z^2} - \gamma H(\varphi - \theta) \tag{24}$$

Since the fluid and solid phases are not in thermal equilibrium, the use of appropriate thermal boundary condition may pose a difficulty. However, the assumption that the solid and fluid phases have equal temperatures at the boundary surfaces made at the beginning of this section helps in overcoming this difficulty. Accordingly, equations (22) to (24) are solved impermeable isothermal boundaries. Hence the boundary conditions are

$$\omega = \frac{\partial \omega}{\partial z} = \theta = \varphi = 0 \text{ at } z = 0, 1 \tag{25}$$

2.3. Linear stability analysis

To study the linear stability theory, we use the linearized version of equations (22) to (24). The principle of exchange of stabilities holds in the presence of isotropy and non-LTE effects (there is only one destabilizing agency) so that the onset of convection is stationary (i.e. $\omega = 0$). We seek the solutions to the linearized equations in the form

$$[w, \theta, \varphi] = [W(z), \Theta(z), \Phi(z)]\, e^{i(lx+my)\sin\pi z + \omega t} \tag{26}$$

Here l, m is the wave numbers in horizontal plane and ω is growth rate. Infinitesimal perturbation of the rest state may be either damp or grow depending on the values of the parameter ω. Substituting the equations (25) in the equations (22) to (24) we get the following equations

$$\left[\frac{\omega}{Pr_D}(a^2 - D^2) - (Ta)^{1/2}D^2 + (a^2 - D^2)\right]W -$$
$$\left[R_A + 2R_M\left\{-\frac{Q_f}{2}z^2 + \left(\frac{Q_f}{2} - 1\right)z + 1\right\}\right]a^2\Theta = 0 \tag{27}$$

$$\left(-Q_f z + \frac{Q_f}{2} + 1\right)W + \left(\omega + a^2 + H - D^2\right)\Theta - H\Phi = 0 \tag{28}$$

$$\gamma H\Theta + \left(\alpha\omega + a^2 + \gamma H - D^2\right)\Phi = 0 \tag{29}$$

The eigenvalue problem associated with the equations (27)–(29) in a horizontal fluid layer bounded by two rigid walls, governing the stability of the basic motion against normal mode perturbations, deduced has the form. We use Galerkin's technique to solve the Eigen value problem. In the Galerkin approach used here the basis (trial) functions satisfy the boundary conditions. In this case, the simplest choice seems to be to write W, Φ and Θ as

$$W_1 = z^3(1 - z)^2, \quad \Theta = \Phi = z(1 - z) \tag{30}$$

With this choice (30), the unknown functions W, ϕ and Θ satisfy the boundary conditions (25) and integrating the equations, so obtained over the layer from 0 to 1, we get

$$\left[\frac{a^2}{66} + \left\{(Ta)^{\frac{1}{2}} + 1\right\}\frac{2}{9}\right]A_1 - \left[\frac{R_A}{2} + R_M\left\{\frac{Q_f + 14}{36}\right\}\right]a^2 B_1 = 0 \tag{31}$$

$$(18 - Q_f)A_1 - 168(a^2 + H + 10)B_1 + 168HC_1 = 0 \tag{32}$$

$$-\gamma H B_1 + (a^2 + \gamma H + 10)C_1 = 0 \tag{33}$$

Now to solve R_A the above equations (31)-(33) can be put in the form of the following matrix, we get

$$\begin{bmatrix} \frac{a^2}{66} + \{(Ta)^{1/2} + 1\}\frac{2}{9} & -\left[R_A + R_M\left\{-\frac{Q_f}{2}z^2 + \left(\frac{Q_f}{2} + 1\right)z + 1\right\}\right]a^2 & 0 \\ 18 + Q_f & -168\left(a^2 + H + 10\right) & 168H \\ 0 & -\gamma H & a^2 + \gamma H + 10 \end{bmatrix}\begin{bmatrix} A_1 \\ B_1 \\ C_1 \end{bmatrix} = \begin{bmatrix} 0 \\ 0 \\ 0 \end{bmatrix} \tag{34}$$

By setting the determinant of the coefficient matrix (34) to zero, we get

$$R_A = \frac{448(a^2 + 10)}{a^2(18 + Q_f)}\left[\frac{a^2}{22} + \{(Ta)^{1/2} + 1\}\frac{2}{3}\right]\left[1 + \frac{H}{a^2 + \gamma H + 10}\right] - \frac{2}{9}R_M(Q_f + 14) \tag{35}$$

3. Result analysis

The impact of internal heating and density maximum in a rotating Darcy-Brinkman porous medium of convection has been investigated using Galerkin method. This study is concentrated to steady state of convection because oscillatory mode seems to be highly implausible. Rayleigh number Eq. (35) is used to determine the stability of the system. If the Rayleigh number is below or above the critical value then the flow is laminar or turbulent. Figs. 2(a) to 2(e) shows that the marginal curves are connected in topological sense and thus the linear stability is calculated in terms of critical Rayleigh number. The system is stable below this critical Rayleigh number and unstable above this number. Figs. 2(a) and 2(e) show the graph of neutral curves for different values of Ta, N, Q_f, R_M, and γ. We observe that there is no change in the topological connectedness of the curves which shows the neutral nature of these curves. Figs. 3(a) to 3(c) exhibit the effect of N against critical Rayleigh number R_A for distinct values of γ, Ta and Q_f. Figs. 3(a) and 3(c) discloses that R_A is decreasing with increase in γ, and Q_f, as N represents the transfer of heat between the fluid and solid phases. If N is very small indicates that there is almost zero transfer of heat between the two phases on the other hand if N is very large indicates there is a rigorous transfer of heat between the two phases. The behavior of the critical Raleigh number points out that the effect of conductivity ratio and internal heat generator of fluid phase is to destabilize the onset of convection. This is because when the conductivity ratio increases the fluid part of the medium gains more heat from the solid phase which leads to begin the convection sooner and thereby, the critical Rayleigh number decreases. When the critical Rayleigh number decreases it implies that the system is coming closer to destabilized mode. The same effect is observed for the case of internal heat generation which is shown in Fig. 3(b). The increase in the internal heat generation causes the fluid phase to acquire more heat and thus convection starts early. It is also noted that R_A is independent of γ when heat transfer is very less and independent of N when γ is very large (≥ 10). Fig. 3(b) shows the effect of Ta versus N on Critical Rayleigh number. It is found that when rotation increases, the values of R_A rise, demonstrating that rotation of fluid has the impact of improving the system's stability. The reason is as the rotation of the porous layer increases there is a slow distribution of heat in the porous layer and fluid particles get heated slowly thus there is a delay in onset of convection which shows that the system is in stable condition.
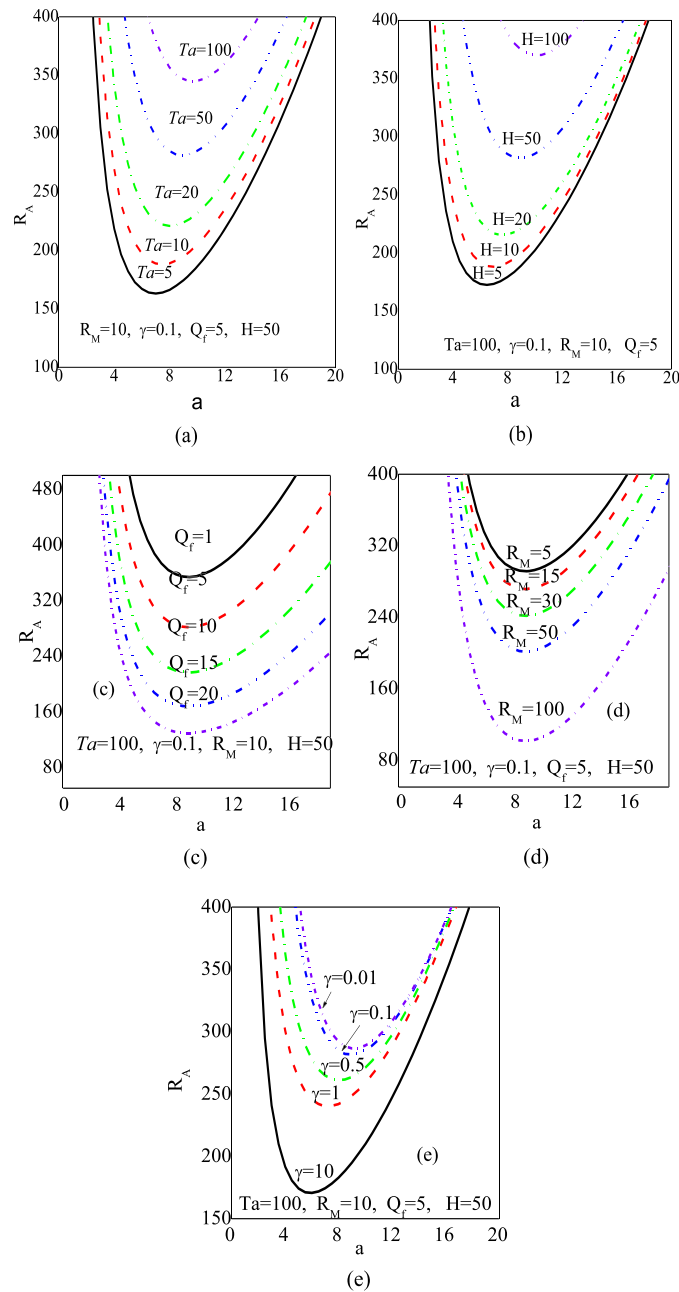
Fig. 2. (a): Neutral stability curves Vs 'a' for different values of Ta. (b): Neutral stability curves Vs 'a' for different values of H. (c): Neutral stability curves Vs 'a' for different values of Q_f. (d): Neutral stability curves Vs 'a' for different values of R_M. (e): Neutral stability curves Vs 'a' for different values of γ.

Figs. 4(a) and 4(b) display the variation of 'a' against N for distinct values of γ and Ta. In Fig. 4(a) it is detected that, for small and large value of N, the critical wave number is not depending on the values of γ. But for intermediate values the critical wave number increase with decrease in γ and attains a maximum. Fig. 4(b) the critical wave number curves increase with increase in Ta, signifying that the impact of Ta is to improve the system stability.

Figs. 5(a) to 5(d) demonstrate the variation of R_A against Q_f for various values of γ, Ta, N and R_M. In Fig. 5(a) the effect of γ on R_A is displayed. It is found that R_A decreases with increase in γ, which shows that the conductivity ratio γ destabilizes the system. In Fig. 5(b) the effect of Ta on the R_A is revealed. It is detected that the R_A increases with increase in Ta, representing that the Taylor number has stabilizing effect. In Fig. 5(c) appear that the effect of Q_f on R_A is presented for various values of N. It is noted that the growing values in Q_f, the values of R_A decline and become zero at some finite value of Q_f. This shows that the Q_f quickens the onset of convection and thus the effect of Q_f causes the instability of the system. In Fig. 5(d) depicted that the R_A decreases as the R_M increases, which indicating that the system turns into unstable mode due to effect of density function.

The comparison presented in Figs. 6(a) and 6(b) is the critical Rayleigh number graphs of present study with the case of Darcy–Benard convection (see Banu and Rees [5]).

Figs. 6(a) and 6(b) are very good comparison of critical Rayleigh numbers with the case Darcy-Benard convection studied by Banu and Rees [5].
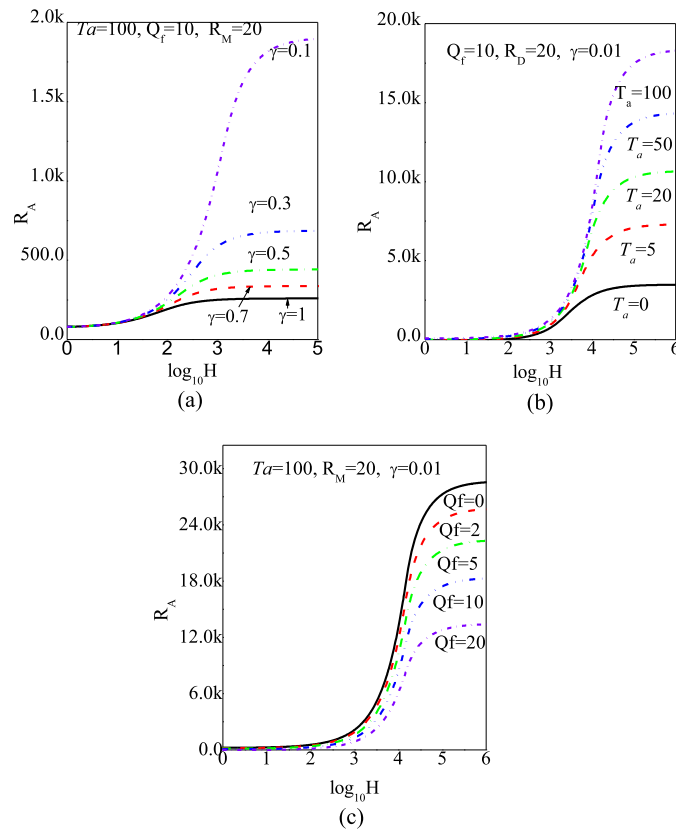
Fig. 3. Variation of R_A against H for different values of γ. (b): Variation of R_A against H for different values of *Ta*. (c): Variation of R_A against H for different values of Q_f.
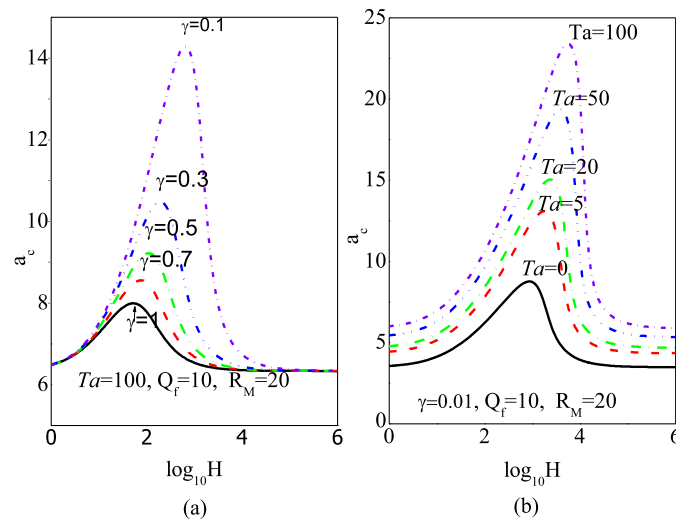

Fig. 4. (a): Variation of 'a' against 'H' for different values of γ. (b): Variation of 'a' against 'H' for different values of *Ta*.

The comparison of critical wavenumber graphs of present study with Darcy–Benard convection done by Banu and Rees [5] is given in Figs. 6(c) and 6(d).

The critical wavenumbers in Figs. 6(c) and 6(d) show the good comparison with the work done by Banu and Rees [5]. Also, the results obtained are presented in Tables 1 and 2, shows a favorable agreement of present work with the results of Banu and Rees [5] in the absence of rotation, internal heat generation and maximum density function thus give confidence that the numerical results obtained are accurate.

4. Conclusion

The stability of a fluid saturated rotating porous layer with internal heat generation and density maximum is studied when both fluid and solid phases have different temperatures. Galerkin method is used to find the Eigen values of the problem. The effect of internal heat generation, rotation and conductivity ratio is determined and demonstrated graphically. The following conclusions have been drawn point by point:
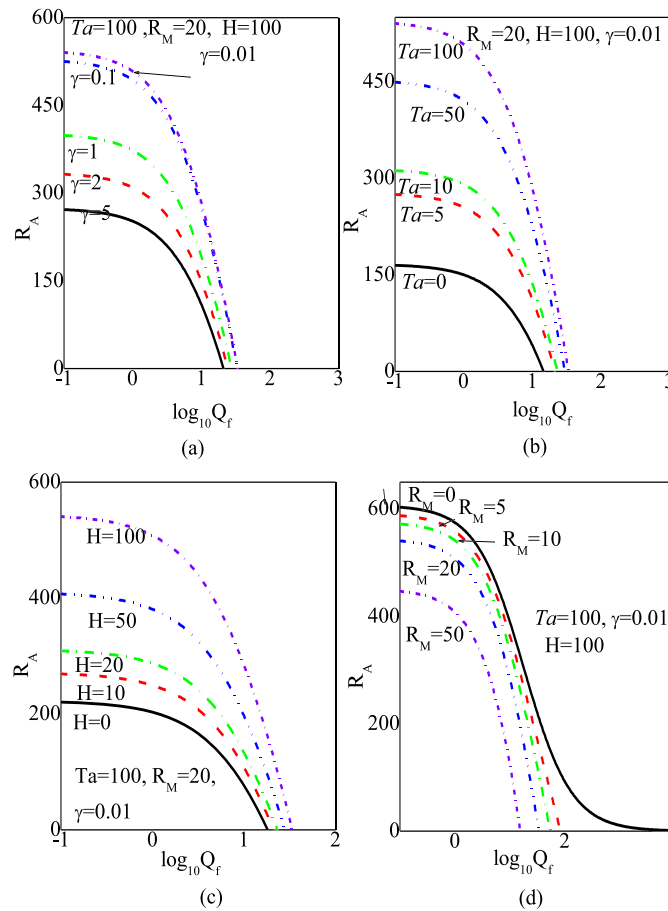
Fig. 5. (a): Plots of R_A versus Q_f for different values of γ. (b): Plots of R_A versus Q_f for different values of Ta. (c): Plots of R_A versus Q_f for different values of H. (d): Plots of R_A versus Q_f for different values of R_M.

Table 1. Comparison of the critical Rayleigh number of present study with the case of Darcy–Benard convection done by Banu and Rees [5] in the absence of rotation, internal heat generation and maximum density function.

Variation of critical Rayleigh number versus logH for specific values of γ							
H	Critical Rayleigh number obtained for the case of present study				Critical Rayleigh number obtained by Banu and Rees [5]		
	$\gamma = 0.1$	$\gamma = 0.3$	$\gamma = 0.5$	$\gamma = 1$	$\gamma = 0.1$	$\gamma = 0.3$	$\gamma = 0.5$	$\gamma = 1$
-2	39.50864	39.50863	39.50863	39.50863	39.50871	39.50870	39.50870	39.50870
-1	39.69856	39.69833	39.69811	39.69755	39.68835	39.68815	39.68795	39.68745
0	41.56690	41.54569	41.52491	41.47464	41.45493	41.43599	41.41741	41.37239
1	58.14440	56.70393	55.43970	52.90179	57.06386	55.79444	54.66823	52.37010
2	163.2115	118.4482	96.35335	72.67197	156.4227	116.2631	95.33384	72.35688
3	370.3745	163.3230	115.6035	78.24936	366.9394	162.8960	115.4474	78.21098
4	427.0948	170.2972	118.1683	78.90134	426.6959	170.2506	118.1551	78.89954
5	433.6257	171.0306	118.4330	78.96766	433.5968	171.0312	118.4350	78.96963
6	434.2889	171.1044	118.4596	78.97430	434.2979	171.1091	118.4630	78.97663
7	434.3553	171.1118	118.4623	78.97497	434.3680	171.1169	118.4658	78.97733
8	434.3620	171.1125	118.4625	78.97503	434.3750	171.1176	118.4661	78.97740
9	434.3627	171.1126	118.4626	78.97504	434.3757	171.1177	118.4661	78.97741
10	434.3627	171.1126	118.4626	78.97504	434.3758	171.1177	118.4661	78.97741

- The rotation of the porous layer if offering extra strength to the system thereby protecting the structure from instability, whereas the internal heat generation does not support the system in maintaining its strength and thus takes the system from a safe zone to a dangerous zone of destabilization.
- The conductivity ratio and density function also have a negative effect on the system stability i.e., both factors oppose the system stability and conductivity ratio is to advance the onset of convection.
- The effect of rotation of porous layer modified conductivity ratio is to enhance the heat transport.
- The overall conclusion is that the rotation parameter Ta stabilizes the system whereas the internal heat generation, conductivity ratio, and density function are having a destabilizing effect on the onset of convection.
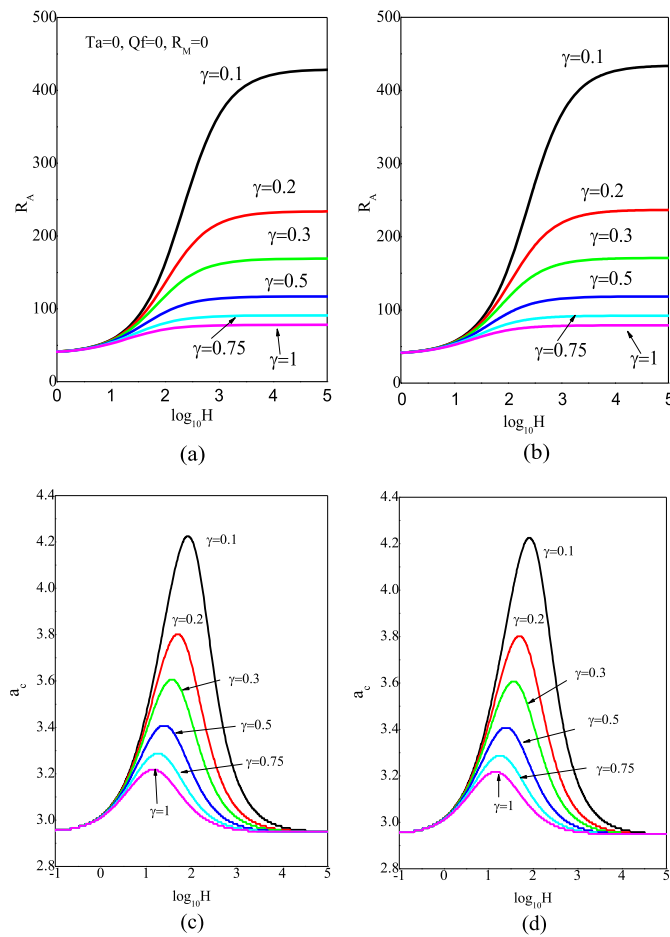
Fig. 6. (a): Variation of R_A v/s H for specific values of γ in present study. (b): Variation of R_A v/s H for different values of γ in DAS Rees et al. result. (c): Variation of ac v/s H for different value of γ in present study. (d): Variation of ac v/s H for different value of γ in Rees et al. result.

Table 2. Comparison of the critical wavenumber of present study with Darcy–Benard convection done by Banu and Rees [5] in the absence of rotation, internal heat generation and maximum density function.

Variation of critical wavenumber versus logH for specific values of g							
H	Present study				Banu and Rees [5]			
	$\gamma = 0.1$	$\gamma = 0.3$	$\gamma = 0.5$	$\gamma = 1$	$\gamma = 0.1$	$\gamma = 0.3$	$\gamma = 0.5$	$\gamma = 1$
-2	3.13958	3.13958	3.13958	3.13958	3.14643	3.14643	3.14643	3.14643
-1	3.14804	3.14804	3.14804	3.14804	3.14643	3.14643	3.14643	3.14643
0	3.14804	3.20662	3.20662	3.19832	3.21714	3.21714	3.21714	3.20936
1	3.14804	3.57378	3.50662	3.39936	3.69459	3.61939	3.55668	3.43511
2	3.14804	3.61783	3.40714	3.24778	4.61519	3.72156	3.46410	3.27109
3	3.14804	3.19832	3.17329	3.14804	3.42783	3.21714	3.18591	3.15436
4	3.14804	3.13958	3.13958	3.13958	3.17017	3.14643	3.14643	3.14643
5	3.14804	3.13958	3.13958	3.13958	3.14643	3.14643	3.13847	3.13847
6	3.14804	3.13958	3.13958	3.13958	3.13847	3.13847	3.13847	3.13847
7	3.14804	3.13958	3.13958	3.13958	3.13847	3.13847	3.13847	3.13847
8	3.14804	3.13958	3.13958	3.13958	3.13847	3.13847	3.13847	3.13847
9	3.14804	3.13958	3.13958	3.13958	3.13847	3.13847	3.13847	3.13847
10	3.14804	3.13958	3.13958	3.13958	3.13847	3.13847	3.13847	3.13847

Declarations

Author contribution statement

N.K. Enagi and Sridhar Kulkarni: Conceived and designed the experiments; Wrote the paper.

Krishna B. Chavaraddi and G.K. Ramesh: Analyzed and interpreted the data; Contributed reagents, materials, analysis tools or data; Wrote the paper.

References

[1] D.A. Nield, A. Bejan, Convection in Porous Media, 3rd ed., Springer, Berlin, 2006.

[2] D.A.S. Rees, I. Pop, Free convection in stagnation point flow in a porous medium using thermal non equilibrium model, Int. Commun. Heat Mass Transf. 26 (1999) 945–954.

[3] D.A.S. Rees, L. Storesletten, A. Postelnicu, The onset of convection in an inclined anisotropic porous layer with oblique principal axes, Transp. Porous Media 62 (2) (2006) 139–156.

[4] S. Govender, P. Vadasz, The effect of mechanical and thermal anisotropy on the stability of gravity driven convection in rotating porous media in the presence of thermal non-equilibrium, Transp. Porous Media 69 (1) (2007) 55–66.

[5] N. Banu, D.A.S. Rees, Onset of Darcy-Benard convection using a thermal non-equilibrium model, Int. J. Heat Mass Transf. 45 (2002) 2221–2228.

[6] M.S. Malashetty, I.S. Shivakumara, S. Kulkarni, The onset of convection in an anisotropic porous layer using a thermal non-equilibrium model, Transp. Porous Media 51 (2005) 1–17.

[7] M.S. Malashetty, I.S. Shivakumara, Sridhar Kulkarni, Convective instability of Oldroyd-B fluid saturated porous layer heated from below using a thermal non-equilibrium model, Transp. Porous Media 64 (2006) 123–139.

[8] M.S. Malashetty, I.S. Shivakumara, S. Kulkarni, The onset of convection in a couple stress fluid saturated porous layer using a thermal non equilibrium model, Phys. Lett. A 373 (7) (2009) 781–790.

[9] M.S. Malashetty, I.S. Shivakumara, S. Kulkarni, The onset of Lapwood-Brinkman convection using a thermal non-equilibrium model, Int. J. Heat Mass Transf. 48 (6) (2005) 1155–1163.

[10] M.S. Malashetty, M. Swamy, S. Kulkarni, Thermal convection in a rotating porous layer using a thermal non-equilibrium model, Phys. Fluids 19 (5) (2007) 054102.

[11] A. Postelnicu, Effect of inertia on the onset of mixed convection in a porous layer using thermal non equilibrium model, J. Porous Media 10 (50) (2007) 515–524.

[12] A.V. Kuznetsov, D.A. Nield, Effect of local thermal non-equilibrium on the onset of convection in a porous medium layer saturated by a nanofluid, Transp. Porous Media 2 (83) (2010) 425–436.

[13] V. Yekasi, S. Pranesh, Effect of suction-injection combination and internal heat source in a fluid with internal angular momentum under 1g and μg, J. Comput. Math. Sci. 9 (6) (2018) 526–537.

[14] B.S. Bhadauria, I. Hashim, P.G. Siddeshwar, Effect of internal heating on weakly nonlinear stability analysis of Rayleigh-Benard convection under g-jitter, Int. J. Non-Linear Mech. 54 (2013) 35–42.

[15] I.S. Shivakumara, M.S. Malashetty, K.B. Chavaraddi, Onset of convection in a visco-elastic-fluid-saturated sparsely packed porous layer using a thermal non equilibrium model, Can. J. Phys. 84 (11) (2006) 973–990.

[16] I.S. Shivakumara, A.L. Mamatha, M. Ravisha, Boundary and thermal non-equilibrium effects on the onset of Darcy-Brinkman convection in a porous layer, J. Eng. Math. 67 (2010) 317–328.

[17] I.S. Shivakumara, A.L. Mamatha, M. Ravisha, Effects of variable viscosity and density maximum on the onset of Darcy-Benard convection using a thermal non equilibrium model, J. Porous Media 13 (7) (2010) 613–622.

[18] Jinho Lee, I.S. Shivakumara, M. Ravisha, Effect of thermal non-equilibrium on convective instability in a ferromagnetic fluid saturated porous medium, Transp. Porous Media 86 (2011) 103–124.

[19] I.S. Shivakumara, Jinho Lee, M. Ravisha, R. Gangadhara Reddy, The onset of Brinkman ferro convection using a thermal non-equilibrium model, Int. J. Heat Mass Transf. 54 (2011) 2116–2125.

[20] I.S. Shivakumara, Jinho Lee, A.L. Mamatha, M. Ravisha, Boundary and thermal non-equilibrium effects on convective instability in an anisotropic porous layer, J. Mech. Sci. Technol. 25 (2011) 911–921.

[21] I.S. Shivakumara, R. Gangadhara Reddy, M. Ravisha, Jinho Lee, Effect of rotation on ferromagnetic porous convection with a thermal non-equilibrium model, Meccanica 49 (2014) 1139–1157.

[22] I.S. Shivakumara, M. Ravisha, C.O. Ng, V.L. Varun, A thermal non-equilibrium model with Cattaneo effect for convection in a Brinkman porous layer, Int. J. Non-Linear Mech. 71 (2015) 39–47.

[23] D. Yadav, J. Wang, Jinho Lee, Onset of Darcy–Brinkman convection in a rotating porous layer induced by purely internal heating, J. Porous Media 20 (8) (2017) 691–706.

[24] S. Sarvanan, Thermal non-equilibrium porous medium with heat generation and density maximum, Transp. Porous Media 76 (2009) 35–43.

[25] R.D. Gaseer, M.S. Kazimi, Onset of convection in a porous media with internal heat generation, J. Heat Transf. 98 (10) (1976) 49–54.

[26] K.B. Chavaraddi, N.K. Enagi, S. Kulkarni, Onset of convection in a couple stress fluid saturated rotating anisotropic porous layers using thermal non-equilibrium model, J. P. J. Heat Mass Transf. 16 (1) (2019) 125–142.

[27] L.S. Lotten, D.A.S. Rees, Onset of convection in an inclined anisotropic porous layer with internal heat generation, Fluids 4 (2019) 75.

[28] C. Israel-Cookey, V.B. Omubo-Peppl, Onset of thermal instability in a low Prandtl number fluid with internal heat source in a porous medium, Am. J. Sci. Ind. Res. 1 (1) (2010) 18–24.

[29] A.K. Srivastava, B.S. Bhadauria, J. Kumar, Magneto convection in an anisotropic porous layer using thermal non-equilibrium model, Special topics & reviews in Porous Media 1 (2) (2011) 1–10.

[30] A. Postelnicu, Effect of inertia on the onset of mixed convection in a porous layer using thermal non-equilibrium model, J. Porous Media 10 (5) (2007) 515–524.

[31] X.J. Xu, Z.B. Xing, F.Q. Wang, Z.M. Cheng, Review on heat conduction, heat convection, thermal radiation and phase change heat transfer of nanofluids in porous media: fundamentals and applications, Chem. Eng. Sci. 195 (2019) 462–483.

[32] M.E.H. Oumar, S.N. Arshika, S. Pranesh, The effect of internal heat generation on the onset of Rayleigh-Benard electro-convection in a micropolar fluid, Int. J. Appl. Eng. Res. 14 (2019) 2327–2335.

[33] C.Q. Wu, H.J. Xu, C.Y. Zhao, A new fractal model on fluid flow/heat/mass transport in complex porous structures, Int. J. Heat Mass Transf. 162 (2020) 120292.

[34] H.J. Xu, Thermal transport in microchannels partially filled with micro-porous media involving flow inertia, flow/thermal slips, thermal non-equilibrium and thermal asymmetry, Int. Commun. Heat Mass Transf. 110 (2020) 104404.

[35] A.A. Yousif, Omar Rafae Alomar, A.T. Hussein, Impact of using triple adiabatic obstacles on natural convection inside porous cavity under non-Darcy flow and local thermal non-equilibrium model, Int. Commun. Heat Mass Transf. 130 (2022) 105760.

[36] Omar Rafae Alomar, Miguel Mendes, D. Trimis, Subhashis Ray, Simulation of complete liquid–vapour phase change process inside porous evaporator using local thermal non-equilibrium model 94 (2015) 228–241.

[37] Omar Rafae Alomar, Analysis of variable porosity, thermal dispersion, and local thermal non-equilibrium on two-phase flow inside porous media 154 (2019) 263–283.

[38] Omar Rafae Alomar, Miguel Mendes, D. Trimis, S. Ray, Numerical simulation of complete liquid–vapour phase change process inside porous media: a comparison between local thermal equilibrium and non-equilibrium models 112 (2017) 222–241.

Krishna B. Chavaraddi, N. K. Enagi and Sridhar Kulkarni

View Online

Export Citation

Non-Equilibrium Thermal Convection in an Anisotropic Porous Layer Saturated with a Viscoelastic Fluid.

Krishna B Chavaraddi[1], N K Enagi[2, 3, a)] and Sridhar Kulkarni[4]

[1]*S.S. Government First Grade College & P.G. Studies Center Nargund-582207, Karnataka, India,*
[2] *Research and Development Centre,Bharathiar University, Coimbatore-641046, Tamilnadu, India*
[3]*KRCE Society's GGD Arts, BMP Commerce, and SVS Science College Bailhongal-591102, Karnataka, India*
[4]*Government First Grade College, Gokak-591307, Karnataka, India*

[a)]Corresponding author:*nkenagi@gmail.com*

Abstract. The study of non-equilibrium thermal convection in an anisotropic porous layer saturated with a visco-elastic fluid is carried out to find how the anisotropy and non-equilibrium of temperature affect the onset of convection. The small perturbation method is applied to obtain the linearized form of equations are then solved by using the normal mode technique. The viscoelasticity is considered by taking Oldrovd-B momentum equation and two separate expressions are used for the energy equation, out of these one represents solid and anther for fluid medium. The effect of both anisotropy and non-equilibrium on the oscillatory and stationary modes of convection has been studied. Apart from these the effect of conductivity ratio, diffusivity ratio, and Darcy Prandtl number is also observed and presented graphically. The stability of the system is protected by thermal anisotropy and diffusivity ratio. But mechanical anisotropy and conductivity ratio are taking the system in destabilizing mode.

Key Words: Thermal Convection, Viscoelastic fluid, Thermal non-equilibrium, Anisotropy.

Nomenclature

a horizontal wavenumber

c specific heat

h height of the layer confined between two free surfaces

g gravitational acceleration

l, m wave numbers in the x and y-direction respectively, $a = \sqrt{l^2 + m^2}$

n   heat transfer coefficient

N   dimensionless heat transfer coefficient, $nh^2/\varepsilon \Bbbk_f$

k   unit vector in Z direction

κ thermal diffusivity, $\frac{\Bbbk}{\rho_0 c}$

K permeability tensor, $K_x(ii + jj) + K_z kk$

$\Bbbk_f, \Bbbk_s$ the tensors representing thermal conductivity for fluid and solid phases.

Pr Darcy Prandtl number, $\upsilon K/\varepsilon \Bbbk_f h^2$

p pressure

$\vec{V}$ velocity vector, (u, v, w)

R_L Rayleigh number, $\frac{g\beta \rho_0 h(\mathcal{T}_\ell - \mathcal{T}_u)K}{\varepsilon \Bbbk_f \mu_f}$

$\mathcal{T}$ temperature

t time

(x, y, z) Coordinates of space

Greek symbols

α diffusivity ratio,$\frac{(\rho_0 c)_s \Bbbk_f}{(\rho_0 c)_f \Bbbk_s} = \frac{\kappa_f}{\kappa_s}$

β thermal expansion coefficient

γ conductivity ratio $\frac{\varepsilon \Bbbk_f}{(1-\varepsilon)\Bbbk_s}$

Γ non dimensional stress relaxation parameter, $\frac{\lambda_1 \Bbbk_f}{(\rho_0 c)_f h^2} = \frac{\lambda_1 \kappa_f}{h^2}$

ε porosity

ξ mechanical anisotropy

μ fluid viscosity

ω frequency

ϕ dimensionless temperature (*solid*)

θ	dimensionless temperature (*fluid*)
ρ	fluid density
$\acute{\lambda}_1$	stress-relaxation time
$\acute{\lambda}_2$	strain-retardation time
Λ	dimensionless retardation to relaxation time ratio, $\acute{\lambda}_2/\acute{\lambda}_1$
μ	dynamic viscosity
ν	kinematics viscosity, μ/ρ_0

Other symbols

| η_f | thermal anisotropy (*fluid*) |

| ∇_1^2 | $\frac{\partial^2}{\partial x^2} + \frac{\partial^2}{\partial y^2}$ |
| ∇^2 | $\nabla_1^2 + \frac{\partial^2}{\partial z^2}$ |

Subscript/ Superscripts

b	base state
ℓ	*lower*
s	*solid phase*
u	upper
f	fluid phase
*	dimensionless quantity
'	perturbed quantity
η_s	thermal anisotropy (*solid*)

INTRODUCTION

Since in many fields such as geothermal energy usage, oil reservoir modeling, building thermal insulation and nuclear waste disposals, the study of convective instability has been motivated by its theatrical and practical importance. As the most theorical works on convective instability has delt with isotropic porous media, but in many circumstances the porous matrix is anisotropic with respect to its mechanical and thermal properties.

The problem of viscoelastic fluid flow through porous medium is the most interesting because it links the complexities of non-Newtonian fluids and porous media and also includes many applications in areas such as science, engineering and technology material processing, petroleum, chemical and nuclear industries, bioengineering and reservoir engineering. Thus, there have been many attempts to find a suitable model to predict the viscoelastic effects in the flows through a porous matrix.

Banu and Rees [1] were reported the Darcy-Benard convection by means of the thermal non-equilibrium model. Chavaraddi et al [2] examined the stability of an anisotropic rotating couple stress fluid in a porous media. Govender [3] has analyzed the results of anisotropy and rotation in a porous media. A detailed study on the thermal non-equilibrium model has been carried out by Malashetty et al [4-6]. Postelnicu [7] studied the nature of inertia on the onset of mixed convection through TNEM. Shivakumara et al [8-9] have investigated the Darcy-Brinkman convection in an anisotropic saturated porous layer using a LTNE. This paper presents the study of convective instability in an anisotropic porous layer with visco-elastic fluid for both oscillatory and stationary modes.

MATHEMATICAL FORMULATION

An anisotropic porous layer of height 'h' with visco-elastic fluid confined between two free surfaces is taken for the study. The lower surface is subjected to heating and the top surface is allowed to cool. Let $\mathcal{T}_\ell$ and $\mathcal{T}_u$ be temperatures at the lower and upper surfaces respectively ($\mathcal{T}_\ell > \mathcal{T}_u$). It is assumed that the temperatures of both solid and fluid medium are not alike except at bounding surfaces so that the use of separate energy equation for both the medium and Darcy-Model to a moment expression yield the better analysis. The physical phenomenon is governed by the following equations,

$$\nabla \cdot \vec{V} = 0 \tag{1}$$

$$\left(1 + \acute{\lambda}_1 \frac{\partial}{\partial t}\right)\left(\frac{\rho}{\varepsilon}\frac{\partial \vec{V}}{\partial t} + \nabla p - \rho g\right) = \frac{\mu}{K}\left(1 + \acute{\lambda}_2 \frac{\partial}{\partial t}\right)\vec{V} \tag{2}$$

$$\varepsilon(\rho_o c)_f \frac{\partial \mathcal{T}_f}{\partial t} + (\rho_o c)_f (\vec{V} \cdot \nabla)\mathcal{T}_f = \varepsilon \Bbbk_{fx}\nabla^2 \mathcal{T}_f + n(\mathcal{T}_s - \mathcal{T}_f) \tag{3}$$

$$(1 - \varepsilon) + (\rho_o c)_s \frac{\partial \mathcal{T}_s}{\partial t} = (1 - \varepsilon)\Bbbk_{sx}\nabla^2 T_s - n(\mathcal{T}_s - \mathcal{T}_f) \tag{4}$$

$$\rho = \rho_o\big[1 - \beta(\mathcal{T}_f - \mathcal{T}_u)\big] \tag{5}$$

To remove pressure term in (2) by operating curl twice on it and render the resulting expressions (3) to (5) dimensionless by using the following transformations

$$(x, y, z) = h(x^*, y^*, z^*), (u, v, w) = \frac{\varepsilon \Bbbk_f}{h(\rho_o c)_f}(u^*, v^*, w^*), p = \frac{\Bbbk_f \mu}{(\rho_o c)_f K}p^* \left.\right\}$$

$$\mathcal{T}_f = (\mathcal{T}_\ell - \mathcal{T}_u)\mathcal{T}_f{}^* + \mathcal{T}_u, \quad \mathcal{T}_s = (\mathcal{T}_\ell - \mathcal{T}_u)\mathcal{T}_s{}^* + \mathcal{T}_u, \quad \mathrm{t} = \frac{(\rho_o c)_f h^2}{k_f} t^* \tag{6}$$

to obtain

$$\left(1 + \Gamma \frac{\partial}{\partial t}\right)\left(\frac{1}{Pr}\frac{\partial \vec{V}}{\partial t} + \nabla p - R_L \mathcal{T}_f\right) = -\left(1 + \Lambda\Gamma \frac{\partial}{\partial t}\right)\vec{V} \tag{7}$$

$$\frac{\partial T_f}{\partial t} + (\vec{V} \cdot \nabla)\mathcal{T}_f = \eta_f \nabla_1^2 \mathcal{T}_f + \frac{\partial^2 T_f}{\partial z^2} + N(\mathcal{T}_s - \mathcal{T}_f) \tag{8}$$

$$\alpha \frac{\partial T_s}{\partial t} = \eta_s \nabla^2 \mathcal{T}_s + \frac{\partial^2 T_s}{\partial z^2} - \gamma N(\mathcal{T}_s - \mathcal{T}_f) \tag{9}$$

Where, $\left.\begin{array}{l} \alpha = \dfrac{(\rho_o c)_s k_{fz}}{(\rho_o c)_f k_{sz}}, \quad \Lambda = \dfrac{\dot\lambda_2}{\dot\lambda_1}, R_L = \dfrac{\rho\beta g\ (\mathcal{T}_l - \mathcal{T}_u)hK}{\varepsilon \mu_f k_f}, \Gamma = \dfrac{\dot\lambda_1 k_f}{(\rho_o c)_f h^2} = \dfrac{\dot\lambda_1 \kappa_f}{h^2} \\[4mm] N = \dfrac{n h^2}{\varepsilon k_{fz}}, \gamma = \dfrac{\varepsilon k_f}{(1-\varepsilon)k_s}, \quad \eta_f = \dfrac{k_{fx}}{k_{fz}}, \quad \eta_s = \dfrac{k_{sx}}{k_{sz}}, \quad \xi = \dfrac{K_x}{K_z} \end{array}\right\} \tag{10}$

Basic State

It is assumed that the basic state is inactive and therefore
$$u = v = w = 0, \quad \mathcal{T}_f = \mathcal{T}_{fb}(z), \quad \mathcal{T}_s = \mathcal{T}_{sb}(z) \tag{11}$$

The temperatures of fluid and solid medium in the basic state satisfies the results
$$\frac{d^2 \mathcal{T}_{fb}}{dz^2} + N(\mathcal{T}_{sb} - \mathcal{T}_{fb}) = 0 \tag{12}$$

$$\frac{d^2 \mathcal{T}_{sb}}{dz^2} - \gamma N(\mathcal{T}_{sb} - \mathcal{T}_{fb}) = 0 \tag{13}$$

with the boundary conditions,
$$\mathcal{T}_{fb} = \mathcal{T}_{sb} = 1 \ \ at \ z = 0, \ \ \mathcal{T}_{fb} = \mathcal{T}_{sb} = 0 \ \ at \ \ z = 1 \tag{14}$$

The basic state solutions satisfying the conditions (14) are
$$\mathcal{T}_{fb} = \mathcal{T}_{sb} = (1 - z) \tag{15}$$

Perturbation State

As there are small disturbances in the basic sate and therefore the temperature and the velocity components under perturbed state are given by
$$(u, v, w) = (\tilde{u}, \tilde{v}, \tilde{w}), \mathcal{T}_f = \mathcal{T}_{fb} + \theta, \mathcal{T}_s = \mathcal{T}_{sb} + \phi \tag{16}$$

Substituting (16) into (7) to (9) with the basic state result we get the perturbed expressions,
$$\left(1 + \Gamma \frac{\partial}{\partial t}\right)\left(\frac{1}{Pr}\frac{\partial}{\partial t}(\nabla^2 \tilde{w}) - R_L \nabla_1{}^2 \theta\right) = -\left(1 + \Lambda\Gamma \frac{\partial}{\partial t}\right)\left(\frac{1}{\xi}\frac{\partial^2 \tilde{w}}{\partial z^2} + \nabla_1^2 \tilde{w}\right) \tag{17}$$

$$\frac{\partial \theta}{\partial t} - \tilde{w} = \eta_f \nabla_1^2 \theta + \frac{\partial^2 \theta}{\partial z^2} + N(\phi - \theta) \tag{18}$$

$$\alpha \frac{\partial \phi}{\partial t} = \eta_s \nabla_1{}^2 \phi + \frac{\partial^2 \phi}{\partial z^2} - \gamma N(\phi - \theta) \tag{19}$$

The hypothesis made in the beginning that the both phases have identical temperatures at the bounding surfaces resolved the difficulty of non-equilibrium thermal condition. Now the equations (17 to 19) are solved for isothermal boundaries. Thus, the end conditions are
$$\left.\begin{array}{l} \tilde{w} = 0 \ \ at \ \ z = 0, \ 1 \\ \theta = \phi = 0 \ \ at \ z = 0, 1 \end{array}\right\} \tag{20}$$

Linear Stability Analysis

The linear version of {(17)-(19)} is used to study the linear stability theory under the boundary conditions (20). The following is the linearized form of equation is used to seek the desired result.

$$[\tilde{w}, \theta, \phi] = [\mathbb{U}(z), \mathbb{V}(z), \mathbb{W}(z)]\, exp\{i(lx + my) + \omega t\} \tag{21}$$

Where $a = \sqrt{l^2 + m^2}$ represents the wave numbers and ω is the growth of disturbance in time 't', which is assumed to be real. Substituting (21) in (17 to 19) we get

$$(1 + \Gamma\omega)\left(\frac{\omega}{Pr}(D^2 - a^2)\mathbb{U} - R_L a^2 \mathbb{V}\right) + (1 + \Lambda\Gamma\omega)\left(\frac{D^2}{\xi} - a^2\right)\mathbb{W} = 0 \tag{22}$$

$$(D^2 - a^2\eta_f - \omega)\mathbb{V} + \mathbb{U} + N(\mathbb{W} - \mathbb{V}) = 0 \tag{23}$$

$$(D^2 - a^2\eta_s - \alpha\omega)\mathbb{W} - \gamma N(\mathbb{W} - \mathbb{V}) = 0 \tag{24}$$

Where $D = \frac{d}{dz}$ now the boundary conditions become

$$\mathbb{U} = \mathbb{V} = \mathbb{W} = 0 \quad for \quad z = 0, 1 \tag{25}$$

Let us assume the solutions to $\mathbb{U}, \mathbb{V}, \mathbb{W}$ are in the form

$$\mathbb{U} = A \sin \pi z, \quad \mathbb{V} = B \sin \pi z, \quad \mathbb{W} = C \sin \pi z \tag{26}$$

Since (26) satisfy the boundary conditions (25) therefore substitute (26) in the equations (22)-(24) we get the following matrix.

$$\begin{bmatrix} \frac{\omega\delta^2\xi}{Pr} + \frac{1+\Gamma\Lambda\omega}{1+\Gamma\omega}B_1 & -R_L a^2\xi & 0 \\ 1 & -(B_2 + \omega + N) & N \\ 0 & \gamma N & -(B_3 + \alpha\omega + \gamma N) \end{bmatrix}\begin{bmatrix} A \\ B \\ C \end{bmatrix} = \begin{bmatrix} 0 \\ 0 \\ 0 \end{bmatrix} \tag{27}$$

Where, $\delta^2 = a^2 + \pi^2$, is the total wave number, $B_1 = \pi^2 + a^2\xi$, $B_2 = \pi^2 + a^2\eta_f$, $B_3 = \pi^2 + a^2\eta_s$

Equating the determinant of the above coefficient matrix to zero we get R_L.

$$R_L = \frac{\left(\frac{\omega\delta^2\xi}{Pr} + \frac{1+\Gamma\Lambda\omega}{1+\Gamma\omega}B_1\right)\left[B_2 + \omega + \frac{N(B_3 + \alpha\omega)}{(B_3 + \alpha\omega + N)}\right]}{a^2\xi} \tag{28}$$

Taking $\omega = i\omega_i$ in equation (28), ignoring imaginary terms in denominator, we get

$$R_L = \Delta_1 + i\omega_i\Delta_2 \tag{29}$$

Where, $\Delta_1 = \dfrac{1}{a^2\xi}\left[\dfrac{\left(\frac{1+\Lambda\Gamma^2\omega^2}{1+\Gamma^2\omega^2}B_1\right)\left(B_2 + \frac{N(B_3^2 + B_3\gamma N + a^2\omega^2)}{(B_3+\gamma N)^2 + a^2\omega^2}\right) - \omega^2\left(\frac{\delta^2\xi}{Pr} + \frac{(\Gamma\Lambda-1)}{1+\Gamma^2\omega^2}B_1\right)}{\left(1 + \frac{\alpha\gamma N^2}{(B_3+\gamma N)^2 + a^2\omega^2}\right)}\right]$

$$\tag{30}$$

$$\Delta_2 = \frac{1}{a^2\xi}\left[\begin{array}{c}\left(\frac{1+\Lambda\Gamma^2\omega^2}{1+\Gamma^2\omega^2}B_1\right)\left(1 + \frac{\alpha\gamma N^2}{(B_3+\gamma N)^2 + a^2\omega^2}\right) + \left(B_2 + \frac{N(B_3^2 + B_3\gamma N + a^2\omega^2)}{(B_3+\gamma N)^2 + a^2\omega^2}\right) \\ \left(\frac{\delta^2\xi}{Pr} + \frac{(\Gamma\Lambda-1)}{1+\Gamma^2\omega^2}B_1\right)\end{array}\right] \tag{31}$$

Since R_L is a constant, it must be real. Thus, by (29) it follows that either $\omega_i = 0$ (stationary) or $\Delta_2 = 0$ ($\omega_i \neq 0$, oscillatory).

i)   Stationary Mode

The onset becomes steady if $\omega_i = 0$ then (29) reduces to

$$R_{L,St} = \frac{B_1}{a^2\xi}\left(B_2 + \frac{B_3 N}{B_3 + \gamma N}\right) \tag{32}$$

ii) Oscillatory Mode

For oscillatory mode $\Delta_2 = 0$ ($\omega_i \neq 0$) and hence this yields quadratic polynomial of the form

$$b_1(\omega_i^2)^2 + b_2\omega_i^2 + b_3 = 0 \tag{33}$$

$$\text{Then } \omega^2 = \frac{-b_2 \mp \sqrt{b_2^2 - 4b_1 b_3}}{2b_1} \tag{34}$$

Where $b_1 = a^2\Gamma^2\delta^2\xi + Na^2\Gamma^2\delta^2\xi + Pra^2\Gamma^2\Lambda B_1$

$b_2 = a^2\delta^2\xi + Na^2\delta^2\xi + Pra^2 B_1 + Pra^2\Gamma B_1(\Lambda - 1) + NPra^2\Gamma B_1(\Lambda - 1) + Pr\alpha\gamma N^2\Gamma^2\Lambda B_1 + Pr\gamma N^2\Gamma^2\Lambda B_1 + \gamma\delta^2 N^2\Gamma^2\xi B_2 + \gamma\delta^2 N^2\Gamma^2\xi B_3 + 2Pr\gamma N\Gamma^2\Lambda B_1 B_3 + 2\gamma N\Gamma^2\delta^2\xi B_2 B_3 + N\Gamma^2\delta^2\xi B_3^2 + Pr\Gamma^2\Lambda B_1 B_3^2 + \Gamma^2\delta^2\xi B_2 B_3^2$

$$b_3 = Pr\alpha\gamma N^2 B_1 + Pr\gamma N^2 B_1 + \gamma\delta^2 N^2 \xi B_2 + \gamma N^2 \delta^2 \xi B_3 + 2Pr\gamma N B_1 B_3 + (\Lambda - 1)\big[Pr\gamma N^2 \Gamma B_1 B_3 +$$
$$2\gamma N\delta^2 \xi B_2 B_3 + Pr\gamma N\Gamma B_1 B_2 B_3 + N\delta^2 \xi {B_3}^2 + Pr\gamma N^2 \Gamma B_1 B_2 + Pr B_1 {B_3}^2 + Pr N\Gamma B_1 {B_3}^2 + \delta^2 \xi B_2 {B_3}^2 +$$
$$Pr\Gamma B_1 B_2 {B_3}^2\big]$$

If $\Lambda > 1$ then $b_2 > 0$ and $b_3 > 0$. Thus (33) will not have any positive roots. But (33) has positive roots.

If $\Lambda < 1$ this is the necessary condition for oscillatory onset.

If $\Delta_2 = 0$ then (29) becomes

$$R_L^{Osc} = \left[\frac{\left(\frac{1+\Lambda\Gamma^2\omega^2}{1+\Gamma^2\omega^2}B_1\right)\left(B_2 + \frac{N\left({B_3}^2 + B_3\gamma N + \alpha^2\omega^2\right)}{(B_3+\gamma N)^2 + \alpha^2\omega^2}\right) - \omega^2\left(\frac{\delta^2\xi}{Pr} + \frac{(\Gamma\Lambda - 1)}{1+\Gamma^2\omega^2}B_1\right)}{\left(1 + \frac{\alpha\gamma N^2}{(B_3+\gamma N)^2 + \alpha^2\omega^2}\right)} \right] \quad (35)$$

RESULT ANALYSIS

The expression (32) representing the stationary Rayleigh number is found to be free from the viscoelastic parameters, therefore it is the case of anisotropic porous layer saturated with Newtonian fluid investigated by Malashetty et al [6]. Expression (35) represents oscillatory critical Rayleigh number which characterizes the stability of the system. Figure [1(a) to 1(h)] show the graph of Critical Rayleigh number (R_L) versus heat exchange between solid and fluid medium (N) for different values of other parameters. Figure 1(a) displays the outcome of η_s on R_L. In this graph the critical values of the Rayleigh number are found to decrease with a decrease in thermal anisotropy. When thermal anisotropy is less means that the conductivity of solid phase along horizontal direction is lesser than the conductivity in the vertical direction which yields to increase in the critical Rayleigh number. The same result is observed in the case of effect of thermal anisotropy for fluid medium in figure 1(b), because the conductivity property is same for both fluid and solid medium. Figure 1(c) shows the variation of R_L with N. It is observed that when the transfer of heat between the solid and fluid media is at the beginning stage i.e when N is very small almost equal to zero, then the two curves remain unchanged for different values of conductivity ratio γ this is because when heat transfer between the two media is almost zero, the porous medium acquire minimum heat and conductivity ratio does not affect the basic properties of the medium. Therefore, the conductivity ratio does not affect the heat transfer process for small N. But one can observe this behavior disappears for large values of N corresponds to transfer of heat between the two media to a greater extent. Therefore, for large values of N the critical Rayleigh number decreases with an increase in conductivity ratio. Figure 1(d) shows the change in R_L with N for different values of ξ. In this graph, the values of the critical Rayleigh number are decreasing with an increase in mechanical anisotropy. It is observed that the critical Rayleigh number is constant for very small values of N and increases slowly, reaches maximum and takes asymptotic values depending on the values of ξ for large values of N. This is understood as varying horizontal permeability and keeping vertical permeability fixed the increased horizontal permeability reduces R_L.

Figure 1(e) displays the result of dimensionless stress relaxation time Γ on the onset for a fixed value of the other dimensionless terms. In this case the critical value of R_L decreases with an increase in the value of Γ. Figure 1(f) illustrate the effect of Pr on R_L. It is found that the increase in the value of Prandtl number is to decrease the value of R_L and thus makes the system more unstable. Figure 1(g) displays the impact of α on R_L. We observe that an increase in the value of α increases the critical value of R_L for the oscillatory mode. The result of Λ, the retardation-to-relaxation-time ratio, on the oscillatory critical Rayleigh number is shown in Fig 1(h). We observe that the critical oscillatory Rayleigh number decreases with decrease in the value of Λ. For very small Λ, that is for $\Lambda \leq 0.01$, the critical oscillatory Rayleigh number is found to be independent of the interphase heat transfer coefficient N.

Figure [2(a) to 2(h)] shows the sequential change in critical wave number against N for both modes of onset with different values of other physical quantities. It is observed that the curves are constant for very small and very large values of N. This happened because, as N tends to zero the solid phase stops the performance of the thermal field of the fluid and when N tends to infinity both phases have alike temperatures. But for intermediate values of N, the critical wave number attains the extremum for each η_s, η_f, γ, ξ, Γ, Λ, α, and Pr. It is also noted that the critical wave number tends to two limits one as N tends to zero and another as N tends to infinity for both modes of onset. But for the moderate values of N the critical wave number is increasing with an increase in values of η_s, η_f, α, and Pr as shown in figure 2(a), 2(b), 2(g) & 2(h), but it is decreasing with an increase in the value of γ, ξ, Γ and Λ as

shown in figure 2(c), 2(d), 2(e) & 2(f) indicating that both thermal anisotropy, diffusivity ratio, Prandtl number have enhanced the stability of the system, whereas the γ, ξ, Γ and Pr make the system unstable.

The impact of N on the critical vale of frequency of the over stable motion for various values of η_s, η_f, Pr, Λ, γ, and α is exhibited in figure [3(a) to 3(f)]. It is observed that the frequency increases with an increase in η_s, η_f and Pr in figures [3(a) to 3(c)] indicating that both the thermal anisotropy of solid and fluid phases and the Prandtl number enhance the stability of the system. But the graph [3(d) to 3(f)] shows that increase in Λ, γ and α decreases critical frequency.
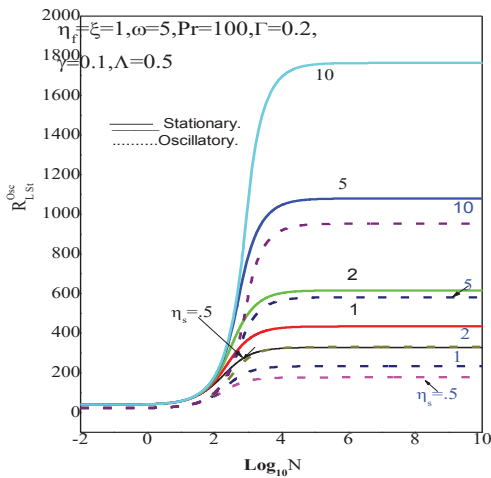
FIGURE 1(a). The effect of H on Rc for different values of η_s
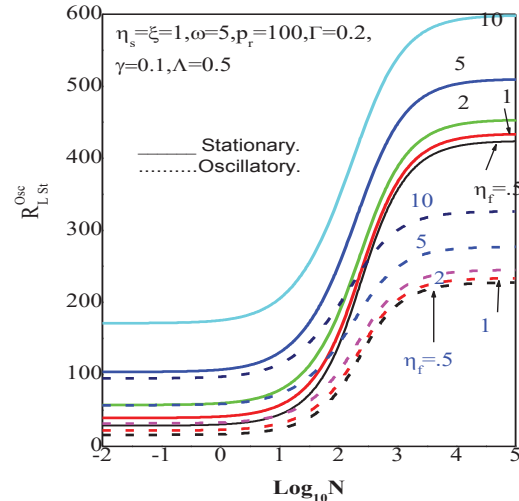
FIGURE 1(b). The effect of H on Rc for different values of η_f
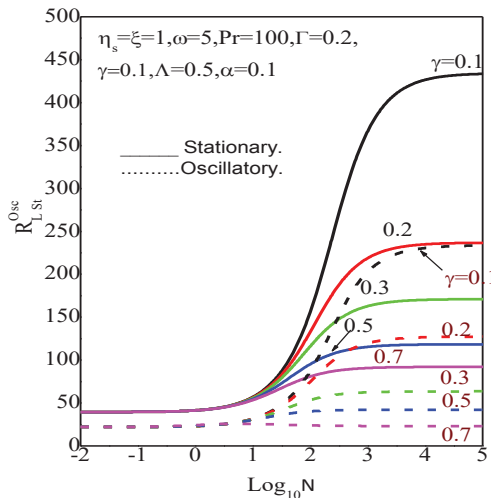
FIGURE 1 (c). The effect of H on Rc for different values of γ
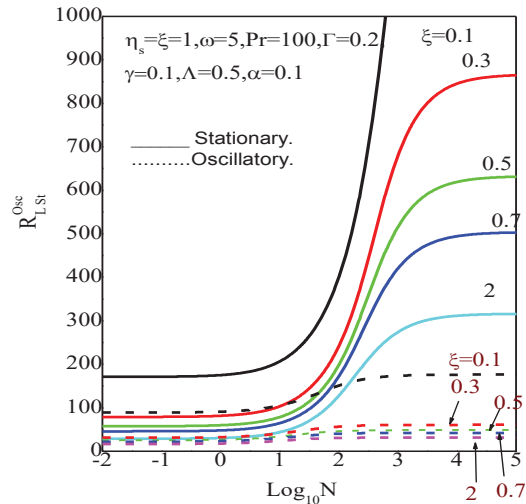
FIGURE 1 (d). The effect of H on Rc for different values of ξ
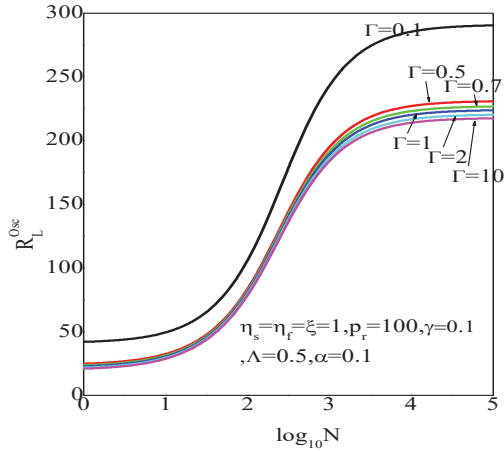
FIGURE 1(e). The effect of N on R_L for different values of Γ
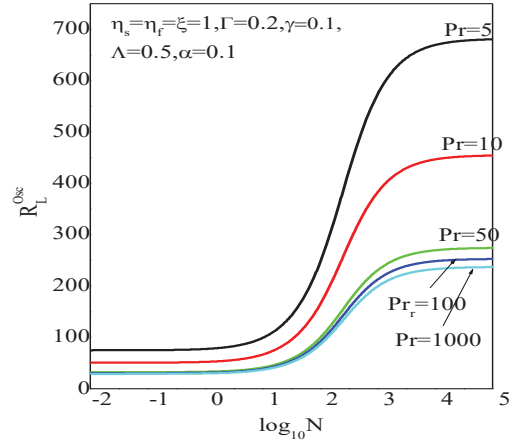
FIGURE 1(f). The effect of N on R_L for different values of Pr
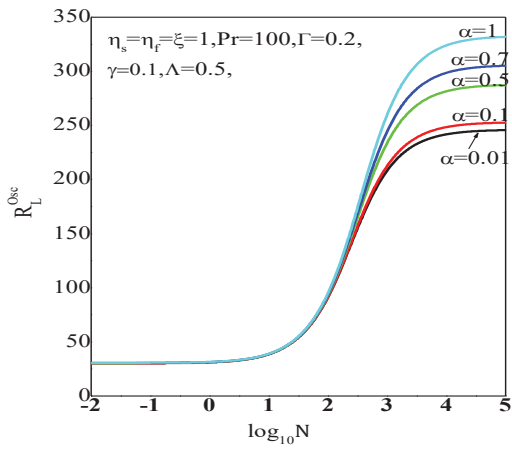
FIGURE 1(g).The effect of N on R_L for different values of α
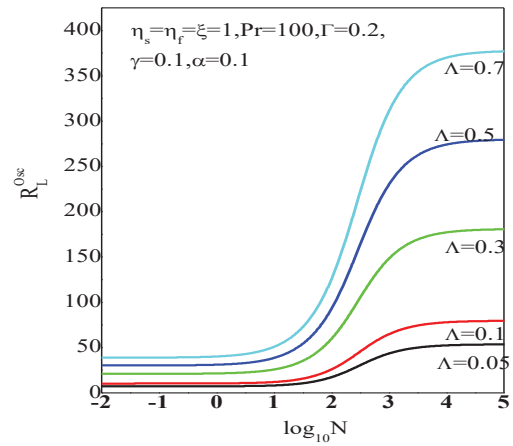
FIGURE 1(h). The effect of N on R_L for different values of Λ
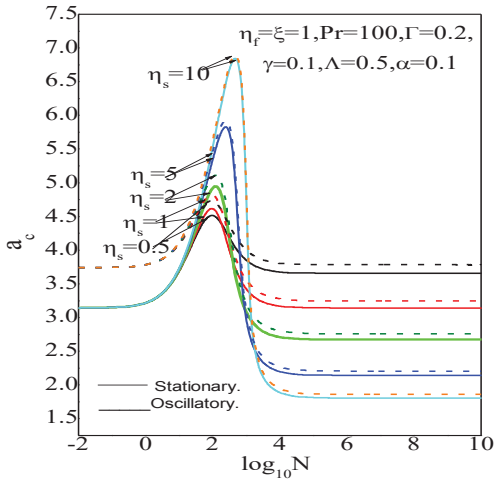
FIGURE 2(a).The effect of H on critical wave number for different values of η_s
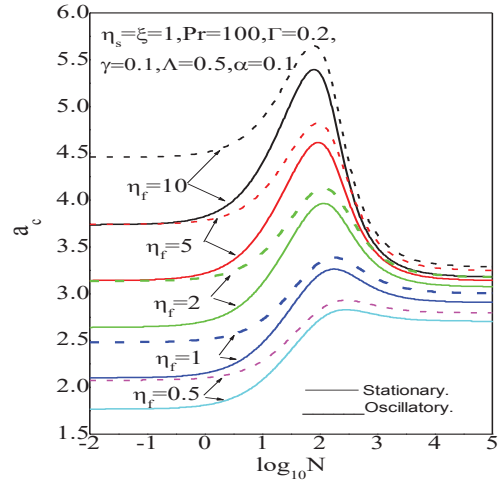
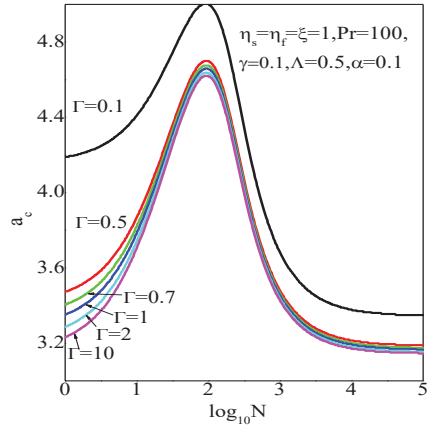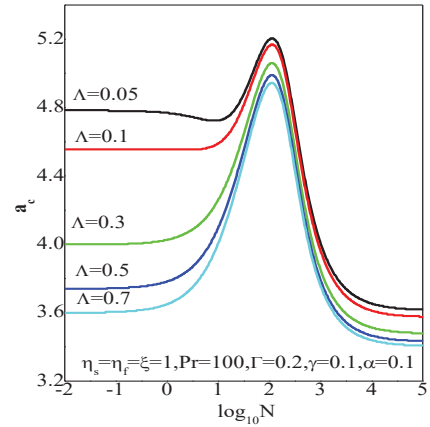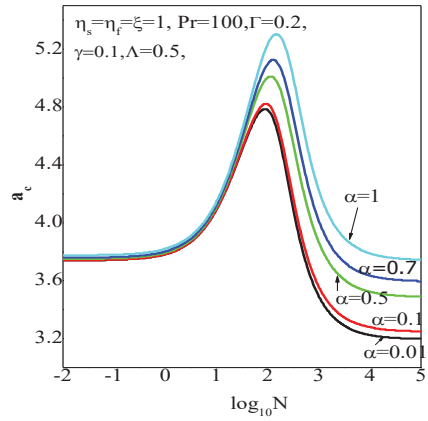**FIGURE 2(b).The effect of H on critical wave number for different values of η_f**
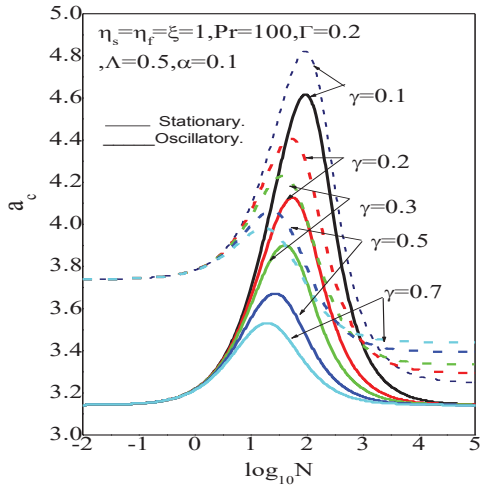
FIGURE 2(c).The effect of H on critical wave number for different values of γ
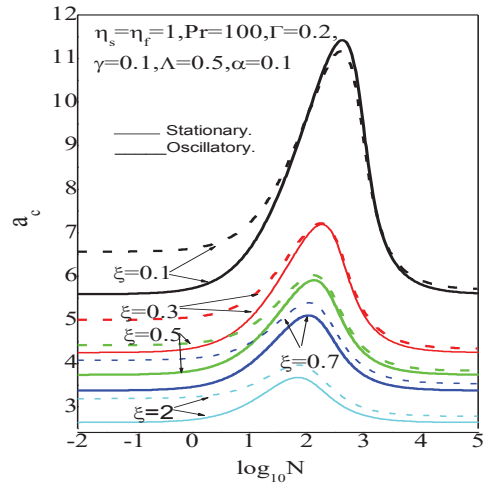
FIGURE 2(d).The effect of H on critical wave number for different values of ξ

FIGURE 2 (e). The effect of N on a_c for different values of Γ

FIGURE 2 (f). The effect of N on a_c for different values of Λ

FIGURE 2 (g). The effect of N on a_c for different values of α
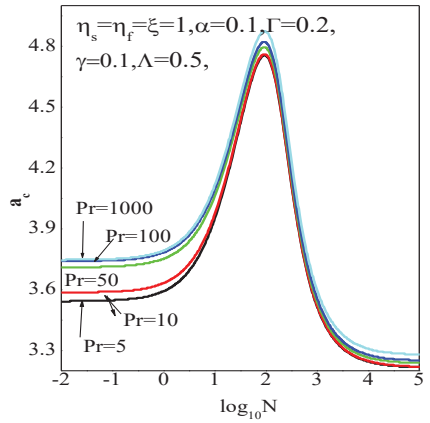
FIGURE 2 (h). The effect of N on a_c for different values of Pr
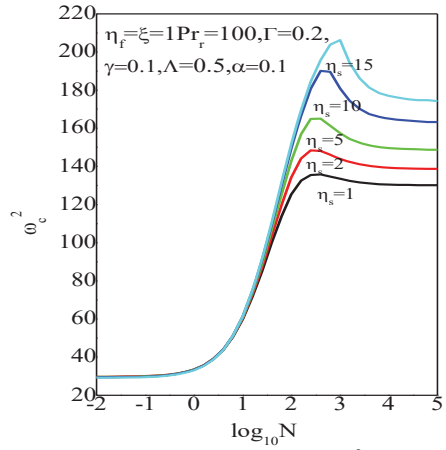
FIGURE 3 (a). Graph of ω_c^2 V/s N for different values of η_s
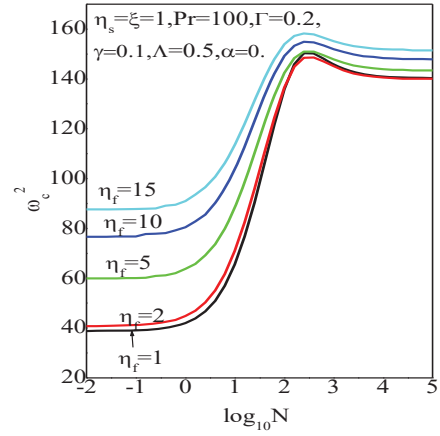
FIGURE 3 (b). Graph of ω_c^2 V/s N for different values of η_f
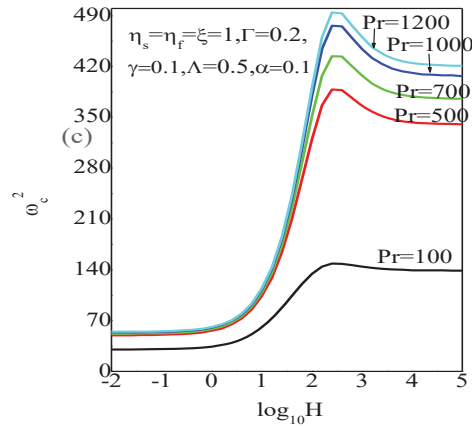
FIGURE 3 (c). Graph of ω_c^2 V/s N for different values of Pr
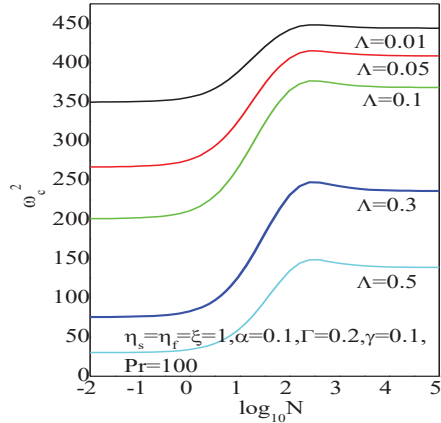
FIGURE 3 (d). Graph of ω_c^2 V/s N for different values of Λ
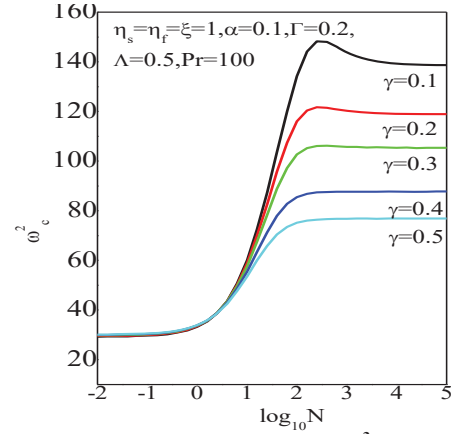
FIGURE 3 (e). Graph of ω_c^2 V/s N for different values of γ
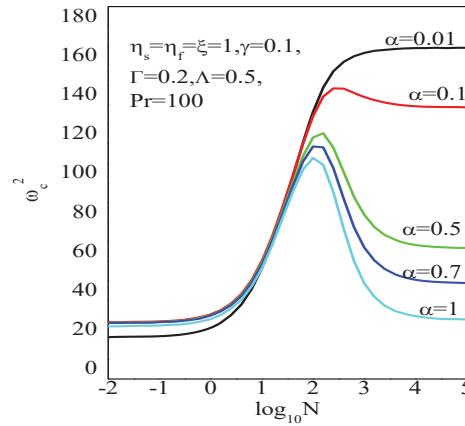

FIGURE 3 (f). Graph of ω_c^2 V/s N for different values of α

CONCLUSION

The non-equilibrium thermal convection in an anisotropic porous layer saturated with a visco-elastic fluid is carried out to find how the anisotropy and non-equilibrium of temperature affect the onset of convection. It is observed that both thermal anisotropies have a positive impact on the stability of the system. That is the thermal anisotropy is making the system stable whereas the conductivity ratio and mechanical anisotropy have a negative impact on the stability of the system, which leads to destabilization. The diffusivity ratio and stress relaxation parameters bring the system in safe mode, whereas the mechanical anisotropy parameter reduces the stability of the system. The retardation-to-relaxation-time ratio will make to start the convection lately.

ACKNOWLEDGEMENT

REFERENCES

1. N. Banu and D.A.S Rees, Int. J. Heat and Mass Transfer. **45,** 2221-2228 (2002).
2. K.B.Chavaraddi, N.K.Enagi and S.Kulkarni, J.P.J of Heat and Mass transfer.**161,** 125-142 (2019).

3. S.Govender, Trans in Porous Media. **643,**413-422 (2006).

4. M.S.Malashetty, I.S.Shivakumara and S.Kulkarni, Trans. in Porous Media. 60(2), 199-215 (2005).

5. M.S.Malashetty, I.S.Shivakumara and Sridhar Kulkarni, Int. J. Heat Mass Transfer. **48**(6), 1155-1163 (2005).

6. M.S.Malashetty, I.S.Shivakumara, Sridhar Kulkarni and Mahantesh Swamy, Trans. in Porous Media. **64**(1), 1231-1239 (2006).

7. A.Postelnicu, J. Porous Media. **10** (50) 515-524 (2007).

8. I.S.Shivakumara, M.S. Malashetty and K.B.Chavaraddi, Can. J. Physics. **84**(11), 973-990 (2006).

9. I.S.Shivakumara, Jinho Lee, A.L.Mamatha and M.Ravisha, J. Mech. Sci. Tech. **25**(4), 911-921 (2011).